Tensor networks, p-adic fields, and algebraic curves: arithmetic and the $\mathbf{AdS_3/CFT_2}$ correspondence

Matthew Heydeman,[*] Matilde Marcolli,[†] Ingmar A. Saberi,[*] and Bogdan Stoica[*]

[*] *Walter Burke Institute for Theoretical Physics,*
California Institute of Technology, 452-48, Pasadena, CA 91125, USA

[†] *Department of Mathematics,*
California Institute of Technology, 253-37, Pasadena, CA 91125, USA

`mheydema@caltech.edu, matilde@caltech.edu, isaberi@caltech.edu,`
`bstoica@theory.caltech.edu`

Abstract

One of the many remarkable properties of conformal field theory in two dimensions is its connection to algebraic geometry. Since every compact Riemann surface is a projective algebraic curve, many constructions of interest in physics (which *a priori* depend on the analytic structure of the spacetime) can be formulated in purely algebraic language. This opens the door to interesting generalizations, obtained by taking another choice of field: for instance, the p-adics. We generalize the AdS/CFT correspondence according to this principle; the result is a formulation of holography in which the bulk geometry is discrete—the Bruhat–Tits tree for $\mathrm{PGL}(2,\mathbb{Q}_p)$—but the group of bulk isometries nonetheless agrees with that of boundary conformal transformations and is not broken by discretization. We suggest that this forms the natural geometric setting for tensor networks that have been proposed as models of bulk reconstruction via quantum error correcting codes; in certain cases, geodesics in the Bruhat–Tits tree reproduce those constructed using quantum error correction. Other aspects of holography also hold: Standard holographic results for massive free scalar fields in a fixed background carry over to the tree, whose vertical direction can be interpreted as a renormalization-group scale for modes in the boundary CFT. Higher-genus bulk geometries (the BTZ black hole and its generalizations) can be understood straightforwardly in our setting, and the Ryu-Takayanagi formula for the entanglement entropy appears naturally.

Contents

1 Introduction

Much attention has been paid of late to ideas that allow certain features of conformal field theory, such as long-range correlations, to be reproduced in lattice systems or other finitary models. As an example, the multiscale entanglement renormalization ansatz (or MERA), formulated by Vidal in [54], provides an algorithm to compute many-qubit quantum states whose entanglement properties are similar to those of the CFT vacuum. In Vidal's method, the states of progressively more distant qubits are entangled using successive layers of a self-similar network of finite tensors.

This tensor network can be thought of as a particular quantum circuit; other new connections between quantum information theory and holography were made in [1], which pointed out that bulk reconstruction and bulk locality in the AdS/CFT correspondence bear strong similarities to the properties of quantum error-correcting codes. This intuition was used in [45] to construct a family of "holographic" quantum codes, associated to hyperbolic tilings. In these codes, bulk qubits are thought of as the logical inputs, the boundary qubits at the periphery of the tiling constitute the encoded state, and the error-correcting properties of the code mimic features of holography such as the Ryu-Takayanagi formula [48].

Given the similarity of these networks (in which the number of tensors scales exponentially with the number of layers) to the geometry of hyperbolic space, it was natural to search for a connection with holography. In [52], Swingle proposed that MERA might be a natural discretization of AdS/CFT, in which the holographic direction (or renormalization scale) corresponds to the successive layers of the tensor network, and individual tensors are associated to "primitive cells" of the bulk geometry. However, successive work [3] identified constraints that prevent an AdS/MERA correspondence of this kind from fully reproducing all features of the bulk physics.

In this paper, we propose that discrete holographic models should be understood as approximating bulk geometry in a fundamentally different way. We are guided by considering a new and orthogonal direction in which the AdS_3/CFT_2 correspondence can be generalized. In these models, based on the p-adic numbers, discrete bulk geometry appears naturally. Despite this, essential and basic features of AdS/CFT, such as bulk isometries and boundary conformal symmetry (which are destroyed by a naive discretization), have analogues and can be fully understood in the discrete setting.

The bulk geometries relevant to the AdS_3/CFT_2 correspondence are well understood. The most well-known black hole solution is that of Bañados, Teitelboim, and Zanelli [2]; this solution was generalized to a family of higher-genus Euclidean black holes by Krasnov [31]. These solutions can be understood in general using the technique of *Schottky uniformization*, which presents a higher-genus black hole as the quotient of empty AdS_3 by a particular discrete subgroup of its isometries.

In [40], a holographic correspondence was established for these three-dimensional geometries. This correspondence expresses the conformal two point correlation function on the conformal boundary at

infinity (a Riemann surface X_Γ of genus g) in terms of geodesic lengths in the bulk space (a hyperbolic handlebody $\mathcal{H}_\Gamma$ of genus g). The formula relating the boundary theory to gravity in the bulk is based on Manin's result [36] on the Arakelov Green's function.

However, we consider AdS$_3$/CFT$_2$ not merely because it is a simple setting for holography. For us, the crucial property of conformal field theory in two dimensions is its strong ties to algebraic geometry. These occur because every compact Riemann surface is a projective algebraic curve, so that many of the analytic concepts that arise in physics can (in two-dimensional contexts) be reformulated in purely algebraic terms. Once a concept can be formulated algebraically, it has many natural generalizations, obtained by changing the field of numbers one is considering. For instance, given a Riemann surface as the zero locus of a polynomial equation with rational coefficients, one can ask for the set of solutions over $\mathbb{C}$, over $\mathbb{R}$, over more exotic fields like the p-adics, or even over the integers.

The aforementioned holographic formula—and the the whole geometric setting of the correspondence, consisting of the Euclidean hyperbolic space AdS$_3$, its conformal boundary $\mathrm{P}^1(\mathbb{C})$, and quotients by actions of Schottky groups $\Gamma \subset \mathrm{PSL}(2,\mathbb{C})$—has a natural analogue in which the field is the p-adic numbers $\mathbb{Q}_p$. The bulk space becomes the Bruhat–Tits tree of $\mathbb{Q}_p$, which is a manifestly discrete infinite graph of uniform valence. Its conformal boundary at infinity is $\mathrm{P}^1(\mathbb{Q}_p)$, which can be thought of as the spacetime for an unusual class of CFTs. Black hole solutions are understood to be quotients of this geometry by p-adic Schottky groups $\Gamma \subset \mathrm{PGL}(2,\mathbb{Q}_p)$; these are known as *Mumford curves* in the mathematics literature. The results of Drinfeld and Manin [35] on periods of p-adic Schottky groups provide the corresponding holographic formula in this non-archimedean setting. We will give what we hope are intuitive introductions to these possibly unfamiliar concepts in the bulk of the paper.

Conformal field theory on p-adic spacetime has previously been developed, for the most part, in the context of the p-adic string theory (see, for instance, [10] and references therein), but has also been considered abstractly [42]. However, our perspective on the subject will be somewhat different: rather than using the p-adics as a worldsheet to construct real-space string amplitudes, our goal in this paper is to further develop the original holographic correspondence of [40] for the higher-genus black holes, informed by recent developments in the understanding of the AdS/CFT correspondence. We will emphasize the large extent to which algebraic structure allows familiar ideas, concepts, and arguments from ordinary AdS$_3$/CFT$_2$ can be carried over—in many cases line by line—to the p-adic setting. In addition to the holographic formulas of Manin and Marcolli, the standard semiclassical holographic analysis of scalar fields propagating without backreaction in anti-de Sitter space applies almost without alteration to the Bruhat–Tits tree. We discuss this in detail in §4.

In some cases, intuitions about how holography works in the archimedean case are supported even more sharply over the p-adics. For example, one normally thinks of the holographic direction as corresponding

to a renormalization-group scale. Over the p-adics, as shown in §4.4, boundary modes contribute to the reconstruction of bulk functions only up to a height determined by their wavelength, and reconstruct precisely to zero above this height in the tree.

One of the most important new ideas in the AdS/CFT correspondence is the study of entanglement entropy in boundary states and its connection (via the Ryu-Takayanagi formula) to the geometry of the bulk. We argue that, at least for the p-adic free boson CFT, an analogue of the familiar logarithmic scaling of the ground-state entanglement entropy should hold. Given such a formula, the Ryu-Takayanagi formula follows immediately from simple considerations of the geometry of the tree.

Tensor network models are often of interest because they reproduce our expectations about ground-state entanglement entropy, and in some cases (like the holographic quantum code of Pastawski *et al.* [45]) also satisfy formulas similar to Ryu-Takayanagi that relate the entanglement entropy to the size of paths or surfaces in the interior of the network. Given that our models exhibit a discrete bulk spacetime, a Ryu-Takayanagi formula, and a meaningful (and unbroken) group of bulk isometries/boundary conformal mappings, we suggest that the p-adic geometry is the natural one to consider in attempting to link tensor network models to spacetimes. We offer some ideas in this direction in §3.

Finally, on an even more speculative note, it is natural to wonder if the study of p-adic models of holography can be used to learn about the real case. So-called "adelic formulas" relate quantities defined over the various places (finite and infinite) of $\mathbb{Q}$; it was suggested in [38] that fundamental physics should be adelic in nature, with product formulae that relate the archimedean side of physics to a product of the contributions of all the p-adic counterparts. We briefly speculate about adelic formulas for the entanglement entropy in §5; one might hope that such formulas could be used to prove inequalities for entanglement entropy like those considered in [5], using ultrametric properties of the p-adics. We hope to further develop the adelic perspective, and return to these questions, in future work.

2 Review of necessary ideas

2.1 Basics of p-adic numbers

We begin with a lightning review of elementary properties of the p-adic fields. Our treatment here is far from complete; for a more comprehensive exposition, the reader is referred to [32], or to another of the many books that treat p-adic techniques.

When one constructs the continuum of the real numbers from the rationals, one completes with respect to a metric: the distance between two points $x, y \in \mathbb{Q}$ is

$$d(x, y) = |x - y|_\infty, \tag{2.1}$$

where $|\cdot|_\infty$ is the usual absolute value. There are Cauchy sequences of rational numbers for which successive terms become arbitrarily close together, but the sequence does not approach any limiting rational number. The real numbers "fill in the gaps," such that every Cauchy sequence of rational numbers converges to a real limit by construction. That property is known as metric completeness.

The p-adic fields $\mathbb{Q}_p$ are completions of $\mathbb{Q}$ with respect to its other norms; these are defined by

$$\mathrm{ord}_p(x) = n \text{ when } x = p^n(a/b) \text{ with } a, b \perp p; \tag{2.2}$$

$$|x|_p = p^{-\mathrm{ord}_p(x)}. \tag{2.3}$$

By a theorem of Ostrowski, every norm on $\mathbb{Q}$ is equivalent to one of the p-adic norms or the usual (∞-adic) norm. It is common to refer to the different possible completions as the different "places" of $\mathbb{Q}$.

A number is p-adically small when it is divisible by a large power of p; one can think of the elements of $\mathbb{Q}_p$ as consisting of decimal numbers written in base p, which can extend infinitely far *left* (just as real numbers can be thought of as ordinary decimals extending infinitely far *right*). $\mathbb{Q}_p$ is uncountable and locally compact with respect to the topology defined by its metric; as usual, a basis for this topology is the set of open balls,

$$B_\epsilon(x) = \{y \in \mathbb{Q}_p : |x - y|_p < \epsilon\}. \tag{2.4}$$

The ring of integers $\mathbb{Z}_p$ of $\mathbb{Q}_p$ is also the unit ball about the origin:

$$\mathbb{Z}_p = \{x \in \mathbb{Q}_p : |x|_p \leq 1\}. \tag{2.5}$$

It can be described as the inverse limit of the system of base-p decimals with no fractional part and finite (but increasingly many) digits:

$$\mathbb{Z}_p = \varprojlim \left(\cdots \to \mathbb{Z}/p^{n+1}\mathbb{Z} \to \mathbb{Z}/p^n\mathbb{Z} \to \mathbb{Z}/p^{n-1}\mathbb{Z} \to \cdots \right). \tag{2.6}$$

$\mathbb{Z}_p$ is a discrete valuation ring; its unique maximal ideal is $\mathfrak{m} = p\mathbb{Z}_p$, and the quotient of $\mathbb{Z}_p$ by $\mathfrak{m}$ is the finite field $\mathbb{F}_p$. In general, for any finite extension of $\mathbb{Q}_p$, the quotient of its ring of integers by its maximal ideal is a finite field $\mathbb{F}_{p^n}$; we give more detail about this case in §6.1.

2.2 The Bruhat–Tits tree and its symmetries

In this section, we will describe the Bruhat–Tits Tree T_p and its symmetries. It should be thought of as a hyperbolic (though discrete) bulk space with conformal boundary $\mathrm{P}^1(\mathbb{Q}_p)$. Since these trees are a crucial part of the paper and may be unfamiliar to the reader, our treatment is informal, and aims to build
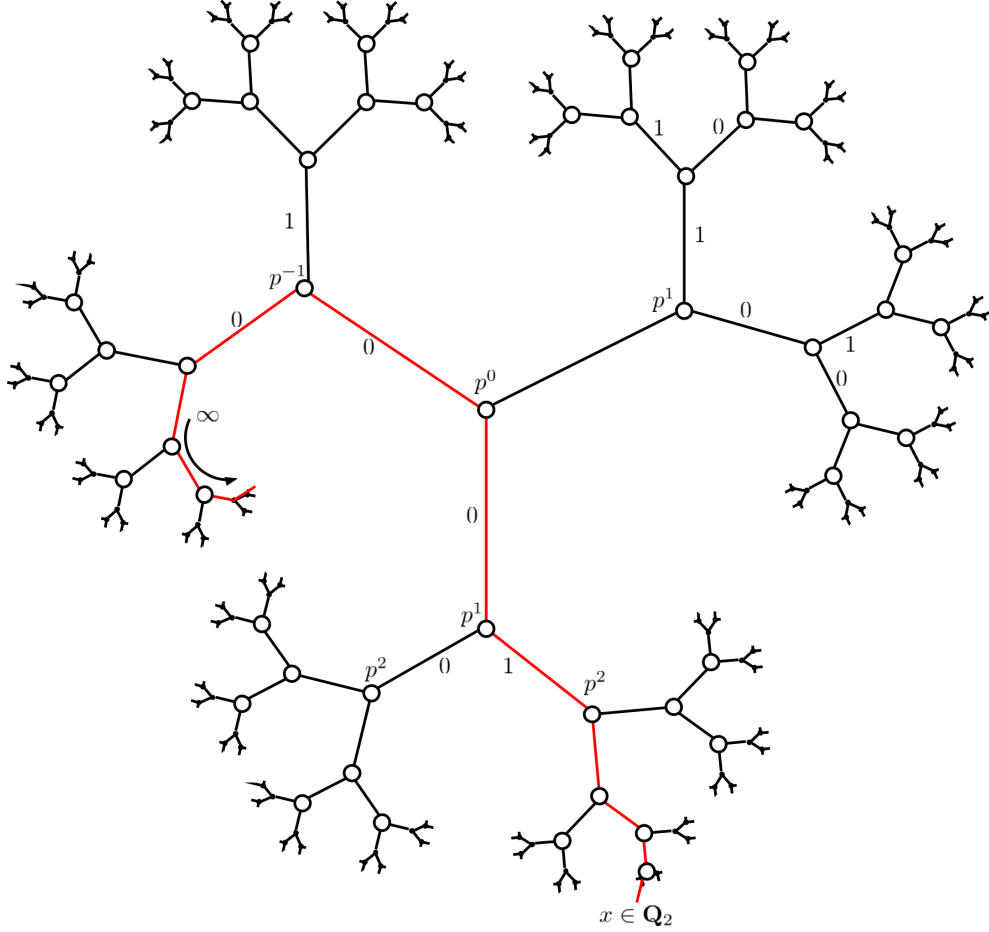
Figure 1: The standard representation of the Bruhat–Tits tree. The point at infinity and the center are arbitrary as the tree is homogeneous. Geodesics such as the highlighted one are infinite paths through the tree from ∞ to the boundary which uniquely specify elements of $\mathbb{Q}_p$. This path as a series specifies the digits of the decimal expansion of $x \in \mathbb{Q}_2$ in this example. At the nth vertex, we choose either 0 or 1 corresponding to the value of x_n in the p^nth term of x. Negative powers of p correspond to larger p-adic norms as we move towards the point ∞.

intuition. Out of necessity, our discussion is also brief; for a more complete treatment, the reader may consult notes by Casselman [17] for constructions and properties related to the tree, or [58] for analysis on the tree and connections to the p-adic string.

We begin with a description of the boundary and its symmetries, which are completely analogous to the global conformal transformations of $\mathrm{P}^1(\mathbb{C})$. We then turn our attention to the bulk space T_p, focusing on its construction as a coset space and the action of $\mathrm{PGL}(2, \mathbb{Q}_p)$ on the vertices. Despite the fractal topology of the p-adic numbers, we will find (perhaps surprisingly) that many formulas from the real or complex cases are related to their p-adic counterparts by the rule $|\cdot|_\infty \to |\cdot|_p$.

2.2.1 Conformal group of $\mathrm{P}^1(\mathbb{Q}_p)$

The global conformal group on the boundary is $\mathrm{SL}(2,\mathbb{Q}_p)$, which consists of matrices of the form

$$A = \begin{pmatrix} a & b \\ c & d \end{pmatrix}, \text{ with } a,b,c,d \in \mathbb{Q}_p, \ ad - bc = 1. \tag{2.7}$$

This acts on points $x \in \mathrm{P}^1(\mathbb{Q}_p)$ by fractional linear transformations,

$$x \to \frac{ax + b}{cx + d}. \tag{2.8}$$

It can be checked that matrix multiplication corresponds to composition of such maps, so that the group action is well-defined. This is analogous to the $\mathrm{SL}(2,\mathbb{C})$ action on the Riemann sphere $\mathrm{P}^1(\mathbb{C})$. (We will sometimes also refer to $\mathrm{PGL}(2,\mathbb{Q}_p)$; the two differ only in minor details.)

The existence of a local conformal algebra for $\mathbb{Q}_p$, in analogy with the Virasoro symmetry in two-dimensional conformal field theory or general holomorphic mappings of $\mathrm{P}^1(\mathbb{C})$, is a subtle question. It is difficult to find definitions of a p-adic derivative or an infinitesimal transformation that are satisfactory for this purpose. In particular, since the "well-behaved" complex-valued functions on $\mathbb{Q}_p$ are in some sense locally constant, there are no interesting derivations that act on the space of fields [42]. In this paper, we will concern ourselves only with global symmetries, which can still be used to constrain the properties of p-adic conformal field theories. We speculate about the possibility of enhanced conformal symmetry in §6.2.

The determinant condition implies that there are three free p-adic numbers which specify an element of $\mathrm{SL}(2,\mathbb{Q}_p)$. A convenient way to decompose a general $\mathrm{SL}(2,\mathbb{Q}_p)$ transformation is to view it as the product of a special conformal transformation, a rotation, a dilatation, and a translation:

$$\begin{pmatrix} p^m a & b \\ c & p^{-m}a^{-1}(1+bc) \end{pmatrix} = \begin{pmatrix} 1 & 0 \\ cp^{-m}a^{-1} & 1 \end{pmatrix} \begin{pmatrix} a & 0 \\ 0 & a^{-1} \end{pmatrix} \begin{pmatrix} p^m & 0 \\ 0 & p^{-m} \end{pmatrix} \begin{pmatrix} 1 & bp^{-m}a^{-1} \\ 0 & 1 \end{pmatrix}, \tag{2.9}$$

where $a,b,c \in \mathbb{Q}_p$ and $|a|_p = 1$. One can verify that the product is an arbitrary element of $\mathrm{SL}(2,\mathbb{Q}_p)$, where the determinant condition has been used to eliminate the d parameter. This represents a translation by $bp^{-m}a^{-1}$, a dilatation by p^{2m}, a rotation by a^2, and a special conformal translation by $cp^{-m}a^{-1}$. We have separated the diagonal subgroup into multiplication by elements of the unit circle, $a \in \mathbb{U}_p \subset \mathbb{Z}_p$, which do not change the p-adic norm (and thus are "rotations" in a p-adic sense), and multiplication by powers of p which scale the p-adic norm (and so correspond to dilatations). Representations of the multiplicative group of unit p-adics provide an analogue of the spin quantum number; we discuss this further in §4.5. It

is worth stressing that these transformations are finite, and so we are characterizing the symmetry group rather than the algebra.

As is often the case in real conformal field theories, we can focus on the dilation subgroup. A diagonal matrix in $\mathrm{SL}(2, \mathbb{Q}_p)$ and its action on the coordinate is

$$\begin{pmatrix} \alpha & 0 \\ 0 & \alpha^{-1} \end{pmatrix}, \quad x \to x' = \alpha^2 x. \tag{2.10}$$

This has the effect of changing the p-adic norm by

$$|x'|_p = |\alpha|_p^2 |x|_p. \tag{2.11}$$

So if $|\alpha|_p \neq 1$, this will scale the size of coordinate. This parallels the complex case in which a dilatation changes the complex norm by $|z'| = |\alpha|^2 |z|$. It will turn out to be the case that 2-point functions of spinless operators in p-adic conformal field theory will depend only on the p-adic norm of their separation. Schematically,

$$\langle \phi(x)\phi(y) \rangle \approx \frac{1}{|x - y|_p^{2\Delta}}. \tag{2.12}$$

Dilations will thus affect correlation functions of the p-adic conformal field theory exactly as in the complex case.

2.2.2 $\mathrm{PGL}(2, \mathbb{Q}_p)$ action on the tree T_p

We have seen that fractional linear transformations of the boundary coordinate work as in the real case. The action of the symmetry on the bulk space T_p is slightly more complicated to describe. Were we working in the archimedean theory, we would identify $\mathrm{PSL}(2, \mathbb{R})$ as the isometry group of the hyperbolic upper half space $\mathbb{H} = \mathrm{SL}(2, \mathbb{R})/\mathrm{SO}(2)$. Here $\mathrm{SO}(2)$ is a maximal compact subgroup. Similarly, in the context of $\mathrm{AdS}_{2+1}/\mathrm{CFT}_2$, we can think of the hyperbolic upper-half 3-space as a quotient space of the isometry group by its maximal compact subgroup: $\mathbf{H}^3 = \mathrm{SL}(2, \mathbb{C})/\mathrm{SU}(2)$.

Following this intuition, we define the *Bruhat–Tits tree* to be the quotient of the p-adic conformal group by its maximal compact subgroup:

$$T_p = \mathrm{PGL}(2, \mathbb{Q}_p)/\mathrm{PGL}(2, \mathbb{Z}_p). \tag{2.13}$$

In contrast with the archimedean examples, T_p is a discrete space: it is a homogeneous infinite tree, with vertices of valence $p + 1$, whose boundary can be identified with the p-adic projective line. We expect isometries to correspond to rigid transformations of the vertices. Formally, the tree represents

the incidence relations of equivalence classes of lattices in $\mathbb{Q}_p \times \mathbb{Q}_p$. As outlined in the appendix of [10], the group $\mathrm{PGL}(2, \mathbb{Q}_p)$ acts by matrix multiplication on the lattice basis vectors and takes one between equivalence classes. These transformations are translations and rotations of the points in the tree; they preserve distances, which are measured in the tree by just counting the number of edges along a given path. Since any two vertices in a connected tree are joined by exactly one path, this is well-defined; all paths are geodesics.

A standard way of representing T_p is depicted in Fig. 1 for the case $p = 2$. This is a regular tree with $p+1$ legs at each vertex; the exponential growth in the number of vertices with distance from a base point reflects the "hyperbolic" nature of distance in the the tree. Since paths are unique, there is a one-to-one correspondence between infinite paths in the tree starting at ∞ and elements of $\mathbb{Q}_p$. (This can be viewed like a p-adic version of stereographic projection.)

The choice of the apparent center and geodesic corresponding to infinity are arbitrary. Just as in the archimedean case, we must fix three boundary points to identify a p-adic coordinate on the projective line, corresponding to 0, 1, and ∞. Once these arbitrary choices are made, the geodesics joining them form a Y in the bulk, whose center is taken to be the centerpoint of the tree. We can then understand the geodesic connecting ∞ to x as labeling the unique p-adic decimal expansion for $x = p^\gamma(x_0 + x_1 p + x_2 p^2 + \dots)$, where each of the x_n take values in $0, 1, \dots p-1$ corresponding to the p possible choices to make at each vertex. Each vertex of the tree is naturally marked with a copy of the finite field $\mathbb{F}_p$, identified with one "digit" of a p-adic number.

Viewing the tree as the space of p-adic decimal expansions may in some ways be more useful than the definition in terms of equivalence classes of lattices. Geometrically moving closer or further from the boundary corresponds to higher or lower precision of p-adic decimal expansions. Even with no reference to quantum mechanics or gravity, we see some hint of holography and renormalization in the tree- a spatial direction in the bulk parameterizes a scale or precision of boundary quantities. This is explored more fully in §4.2.1.

We now illustrate some examples of $\mathrm{PGL}(2, \mathbb{Q}_p)$ transformations on the tree. First note that the choice of the center node is arbitrary. We can take this point to be the equivalence class of unit lattices modulo scalar multiplication. One can show that this equivalence class (or the node it corresponds to) is invariant under the $\mathrm{PGL}(2, \mathbb{Z}_p)$ subgroup, so these transformations leave the center fixed and rotate the branches of the tree about this point.

More interesting is a generator such as

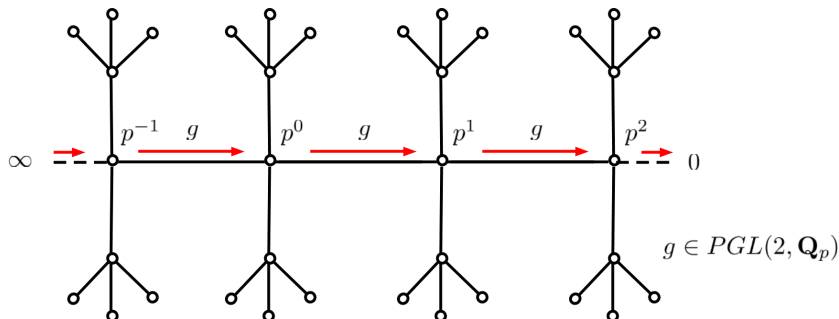$$g = \begin{pmatrix} p & 0 \\ 0 & 1 \end{pmatrix} \in \mathrm{PGL}(2, \mathbb{Q}_p). \tag{2.14}$$

Figure 2: An alternative representation of the Bruhat–Tits Tree (for $p = 3$) in which we have unfolded the tree along the 0 geodesic. The action of elements of $\mathrm{PGL}(2, \mathbb{Q}_p)$ acts by translating the entire tree along different possible geodesics. In this example we translate along the 0 geodesic, which can be thought of as multiplication of each term in a p-adic decimal expansion by p. This map has two fixed points at 0 and ∞. In this "unfolded" form, a point in $\mathrm{P}^1(\mathbb{Q}_p)$ is specified by a geodesic that runs from ∞ and follows the 0 geodesic until some level in the tree where it leaves the 0 geodesic towards the boundary. The p-adic norm is simply p to the inverse power of the point where it leaves the 0 geodesic (so leaving "sooner" leads to a larger norm, and later to a smaller norm.

This transformation (and others in $\mathrm{PGL}(2, \mathbb{Q}_p)$) act by translating the entire tree along a given geodesic (one can see this either from the lattice incidence relations, or from translating or shifting the p-adic decimal series expansion). This is illustrated in Fig. 2. We can think of these transformations as the lattice analogs of translations and dilatations of the real hyperbolic plane.

2.2.3 Integration measures on p-adic spaces

Just as is the case for $\mathbb{C}$, there are two natural measures on $\mathbb{Q}_p$ (or more properly, on the projective line over $\mathbb{Q}_p$); they can be understood intuitively by thinking of $\mathbb{Q}_p$ as the boundary of T_p. The first is the Haar measure $d\mu$, which exists for all locally compact topological groups. With respect to either measure, the size of the set of p-adic integers is taken to be 1:

$$\mu(\mathbb{Z}_p) = 1. \tag{2.15}$$

The Haar measure is then fixed by multiplicativity and translation invariance; any open ball has measure equal to the p-adic norm of its radius. It is helpful to think of $\mathbb{Q}_p$ as being "flat" when considered with this measure.

The other measure, the Patterson-Sullivan measure, is the p-adic analogue of the Fubini-Study metric on $\mathrm{P}^1(\mathbb{C})$. It is most easily defined with reference to the tree, in which we fix a basepoint C (to be thought of as the unique meeting point of the geodesics joining 0, 1, and ∞ when a coordinate is chosen on the boundary). Recall that the open balls in $\mathbb{Q}_p$ correspond to the endpoints of branches of the tree below a

vertex v. In the Patterson-Sullivan measure,

$$d\mu_0(B_v) = p^{-d(C,v)}.\tag{2.16}$$

The two measures are related by

$$\begin{aligned}
d\mu_0(x) &= d\mu(x), && |x|_p \leq 1; \\
d\mu_0(x) &= \frac{d\mu(x)}{|x|_p^2}, && |x|_p > 1.
\end{aligned}\tag{2.17}$$

(Later on, we will at times use the familiar notation dx to refer to the Haar measure.) The most intuitive way to picture the Patterson-Sullivan measure is to imagine the tree pointing "radially outward" from its centerpoint. It is then easy to understand the transformation rule (2.17); it says that when all geodesics point downward from infinity and the boundary is "flat" at the lower end of the picture, points far from zero (outside $\mathbb{Z}_p$) can only be reached by geodesics that travel upward from C before turning back down towards the boundary.

2.3   Schottky uniformization of Riemann surfaces

In this section, we review Schottky uniformization, which allows one to think of a higher-genus Riemann surface as a quotient of the projective line by a particular discrete subgroup of its Möbius transformations.

A Schottky group of rank $g \geq 1$ is a discrete subgroup of $\mathrm{PSL}(2,\mathbb{C})$ which is purely loxodromic and isomorphic to a free group on g generators. The group $\mathrm{PSL}(2,\mathbb{C})$ acts on $\mathrm{P}^1(\mathbb{C})$ by fractional linear transformations,

$$\gamma = \begin{pmatrix} a & b \\ c & d \end{pmatrix} : z \mapsto \frac{az+b}{cz+d}.$$

The loxodromic condition means that each nontrivial element $\gamma \in \Gamma \setminus \{1\}$ has two distinct fixed points $z_\gamma^\pm$ (one attractive and one repelling) in $\mathrm{P}^1(\mathbb{C})$. The closure in $\mathrm{P}^1(\mathbb{C})$ of the set of all fixed points of elements in Γ is the limit set Λ_Γ of Γ, the set of all limit points of the action of Γ on $\mathrm{P}^1(\mathbb{C})$. In the case $g = 1$ the limit set consists of two points, which we can choose to identify with $\{0, \infty\}$, while for $g > 1$ the set Λ_Γ is a Cantor set of Hausdorff dimension $0 \leq \dim_H(\Lambda_\Gamma) < 2$. The Hausdorff dimension is also the exponent of convergence of the Poincaré series of the Schottky group: $\sum_{\gamma \in \Gamma} |\gamma'|^s$ converges for $s > \dim_H(\Lambda_\Gamma)$, [8].

It is well known that any compact smooth Riemann surface X admits a Schottky uniformization, namely $X = \Omega_\Gamma/\Gamma$, where $\Gamma \subset \mathrm{PSL}(2,\mathbb{C})$ is a Schottky group of rank equal to the genus $g = g(X)$ of the Riemann surface, and $\Omega_\Gamma = \mathrm{P}^1(\mathbb{C}) \setminus \Lambda_\Gamma$ is the *domain of discontinuity* of the action of Γ on $\mathrm{P}^1(\mathbb{C})$. There is a well known relation between Schottky and Fuchsian uniformizations of compact Riemann surfaces of

11

genus $g \geq 2$, see [53].

A *marking* of a rank g Schottky group $\Gamma \subset \mathrm{PSL}(2,\mathbb{C})$ is a choice of a set of generators $\{\gamma_1, \ldots, \gamma_g\}$ of Γ and a set of $2g$ open connected regions D_i in $\mathrm{P}^1(\mathbb{C})$, with $C_i = \partial D_i$ the boundary Jordan curves homemorphic to S^1, with the following properties:

1. the closures of the D_i are pairwise disjoint

2. $\gamma_i(C_i) \subset C_{g+i}$

3. $\gamma_i(D_i) \subset \mathrm{P}^1(\mathbb{C}) \setminus D_{g+i}$.

The marking is *classical* if all the C_i are circles. (All Schottky groups admit a marking, but not all admit a classical marking.) A fundamental domain F_Γ for the action of the Schottky group Γ on the domain of discontinuity $\Omega_\Gamma \subset \mathrm{P}^1(\mathbb{C})$ can be constructed by taking

$$F_\Gamma = \mathrm{P}^1(\mathbb{C}) \setminus \cup_{i=1}^g (D_i \cup \bar{D}_{g+i}).$$

This satisfies $\cup_{\gamma \in \Gamma} \gamma(F_\Gamma) = \Omega_\Gamma$. In the case of genus $g = 1$, with $\Gamma = q^{\mathbb{Z}}$, for some $q \in \mathbb{C}$ with $|q| > 1$, the region F_Γ constructed in this way is an annulus A_q, with D_1 the unit disk in $\mathbb{C}$ and D_2 the disk around ∞ given by complement in $\mathrm{P}^1(\mathbb{C})$ of the disk centered at zero of radius $|q|$, so that $q^{\mathbb{Z}} A_q = \mathbb{C}^* = \mathrm{P}^1(\mathbb{C}) \setminus \{0, \infty\} = \Omega_{q^{\mathbb{Z}}}$. The resulting quotient $E_q = \mathbb{C}^*/q^{\mathbb{Z}}$ is the Tate uniformization of elliptic curves.

2.4   Hyperbolic handlebodies and higher genus black holes

The action of $\mathrm{PSL}(2,\mathbb{C})$ by fractional linear transformations on $\mathrm{P}^1(\mathbb{C})$ extends to an action by isometries on the real 3-dimensional hyperbolic space $\mathbf{H}^3$, with $\mathrm{P}^1(\mathbb{C})$ its conformal boundary at infinity. In coordinates $(z, y) \in \mathbb{C} \times \mathbb{R}_+^*$ in $\mathbf{H}^3$, the action of $\mathrm{PSL}(2,\mathbb{C})$ by isometries of the hyperbolic metric is given by

$$\gamma = \begin{pmatrix} a & b \\ c & d \end{pmatrix} : (z, y) \mapsto \left(\frac{(az+b)\overline{(cz+d)} + a\bar{c}y^2}{|cz+d|^2 + |c|^2 y^2}, \frac{y}{|cz+d|^2 + |c|^2 y^2} \right).$$

Given a rank g Schottky group $\Gamma \subset \mathrm{PSL}(2,\mathbb{C})$, we can consider its action on the conformally compactified hyperbolic 3-space $\overline{\mathbf{H}^3} = \mathbf{H}^3 \cup \mathrm{P}^1(\mathbb{C})$. The only limit points of the action are on the limit set Λ_Γ that is contained in the conformal boundary $\mathrm{P}^1(\mathbb{C})$, hence a domain of discontinuity for this action is given by

$$\mathbf{H}^3 \cup \Omega_\Gamma \subset \overline{\mathbf{H}^3} = \mathbf{H}^3 \cup \mathrm{P}^1(\mathbb{C}).$$

The quotient of $\mathbf{H}^3$ by this action is a 3-dimensional hyperbolic handlebody of genus g

$$\mathcal{H}_\Gamma = \mathbf{H}^3/\Gamma,$$

with conformal boundary at infinity given by the Riemann surface $X_\Gamma = \Omega_\Gamma/\Gamma$,

$$\overline{\mathcal{H}}_\Gamma = \mathcal{H}_\Gamma \cup X_\Gamma = (\mathbf{H}^3 \cup \Omega_\Gamma)/\Gamma.$$

Given a marking of a rank g Schottky group Γ (for simplicity we will assume the marking is classical), let D_i be the discs in $\mathrm{P}^1(\mathbb{C})$ of the marking, and let $\mathcal{D}_i$ denote the geodesic domes in $\mathbf{H}^3$ with boundary $C_i = \partial D_i$, namely the $\mathcal{D}_i$ are the open regions of $\overline{\mathbf{H}^3}$ with boundary $S_i \cup D_i$, where the S_i are totally geodesic surfaces in $\mathbf{H}^3$ with boundary C_i that project to D_i on the conformal boundary. Then a fundamental domain for the action of Γ on $\mathbf{H}^3 \cup \Omega_\Gamma$ is given by

$$\mathcal{F}_\Gamma = F_\Gamma \cup (\mathbf{H}^3 \setminus \cup_{i=1}^g (\mathcal{D}_i \cup \bar{\mathcal{D}}_{g+i}).$$

The boundary curves C_i for $i = 1, \ldots, g$ provide a collections of A-cycles, that give half of the generators of the homology of the Riemann surface X_Γ: the generators that become trivial in the homology of the handlebody $\bar{\mathcal{H}}_\Gamma$. The union of fundamental domains $\gamma(\mathcal{F}_\Gamma)$ for $\gamma \in \Gamma$ can be visualized as in Fig. 4.

In the case of genus $g = 1$ with $\Gamma = q^{\mathbb{Z}}$, acting on $\mathbf{H}^3$ by

$$\begin{pmatrix} q^{1/2} & 0 \\ 0 & q^{-1/2} \end{pmatrix} (z, y) = (qz, |q|y),$$

with limit set $\{0, \infty\}$ the fundamental domain $\mathcal{F}_\Gamma$ consists of the space in the upper half space $\mathbf{H}^3$ contained in between the two spherical domes of radius 1 and $|q| > 1$. The generator q of the group acts on the geodesic with endpoints 0 and ∞ as a translation by $\log|q|$. The quotient $\mathbf{H}^3/q^{\mathbb{Z}}$ is a hyperbolic solid torus, with the Tate uniformized elliptic curve $E_q = \mathbb{C}^*/q^{\mathbb{Z}}$ as its conformal boundary at infinity, and with a unique closed geodesic of length $\log q$. It is well known (see [6], [33] and §2.3 of [40]) that the genus one handlebodies $\mathcal{H}_{q^{\mathbb{Z}}}$ are the Euclidean BTZ black holes [2], where the cases with $q \in \mathbb{C} \setminus \mathbb{R}$ correspond to spinning black holes. The geodesic length $\log|q|$ is the area of the event horizon, hence proportional to the black hole entropy.

The case of higher genus hyperbolic handlebodies correspond to generalizations of the BTZ black hole to the higher genus asymptotically AdS_3 black holes considered in [31] and [40].

In these more general higher genus black hole, because of the very different nature of the limit set (a fractal Cantor set instead of two points) the structure of the black hole event horizon is significantly
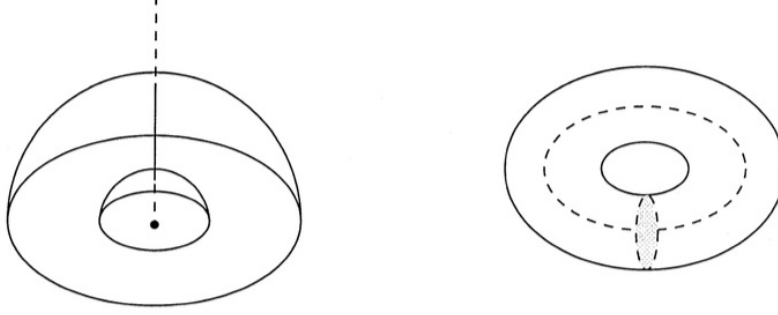
Figure 3: Fundamental domain and quotient for the Euclidean BTZ black hole. Compare with the p-adic BTZ geometry, shown in Fig. 10.

more complicated. In the Euclidean BTZ black hole, the only infinite geodesic that remains confined into a compact region inside the hyperbolic solid torus $\mathcal{H}_{q^{\mathbb{Z}}}$ for both $t \to \pm\infty$ is the unique closed geodesic (the image in the quotient of the geodesic in $\mathbf{H}^3$ given by the vertical line with endpoints 0 and ∞. On the other hand, in the higher genus cases, the geodesics in the hyperbolic handlebody $\mathcal{H}_\Gamma = \mathbf{H}^3/\Gamma$ can be classified as:

1. *Closed geodesics*: these are the images in the quotient $\mathcal{H}_\Gamma$ of geodesics in $\mathbf{H}^3$ with endpoints $\{z_\gamma^+, z_\gamma^-\}$, the attractive and repelling fixed points of some element $\gamma \in \Gamma$.

2. *Bounded geodesics:* these images in the quotient $\mathcal{H}_\Gamma$ of geodesics in $\mathbf{H}^3$ with endpoints on Λ_Γ. If the endpoints are not a pair of fixed points of the same element of Γ the geodesic in the quotient is not closed, but it remains forever confined within a compact region inside $\mathcal{H}_\Gamma$, the *convex core* $\mathcal{C}_\Gamma$.

3. *Unbounded geodesics:* these are images in the quotient $\mathcal{H}_\Gamma$ of geodesics in $\mathbf{H}^3$ with at least one of the two endpoints in Ω_Γ. These are geodesics in $\mathcal{H}_\Gamma$ that wander off (in at least one time direction $t \to \infty$ or $t \to -\infty$) towards the conformal boundary X_Γ at infinity and eventually leave every compact region in $\mathcal{H}_\Gamma$.

The convex core $\mathcal{C}_\Gamma \subset \mathcal{H}_\Gamma$ is the quotient by Γ of the geodesic hull in $\mathbf{H}^3$ of the limit set Λ_Γ. It is a compact region of finite hyperbolic volume in $\mathcal{H}_\Gamma$, and it is a deformation retract of $\mathcal{H}_\Gamma$. A natural replacement for the event horizon of the BTZ black hole in these higher genus cases can be identified in terms of the convex core $\mathcal{C}_\Gamma$, where we think of $\mathcal{C}_\Gamma$ as the region from which geodesic trajectories cannot escape and must remain forever confined. The complement $\mathcal{H}_\Gamma \setminus \mathcal{C}_\Gamma$ is homeomorphic to $\partial\mathcal{C}_\Gamma \times \mathbb{R}_+$ (see [14] for a more general treatment of convex cores of Kleinian groups and ends of hyperbolic 3-manifolds). The boundary $\partial\mathcal{C}_\Gamma$ is the event horizon of the higher genus black hole, with the black hole entropy proportional to the area of $\partial\mathcal{C}_\Gamma$.
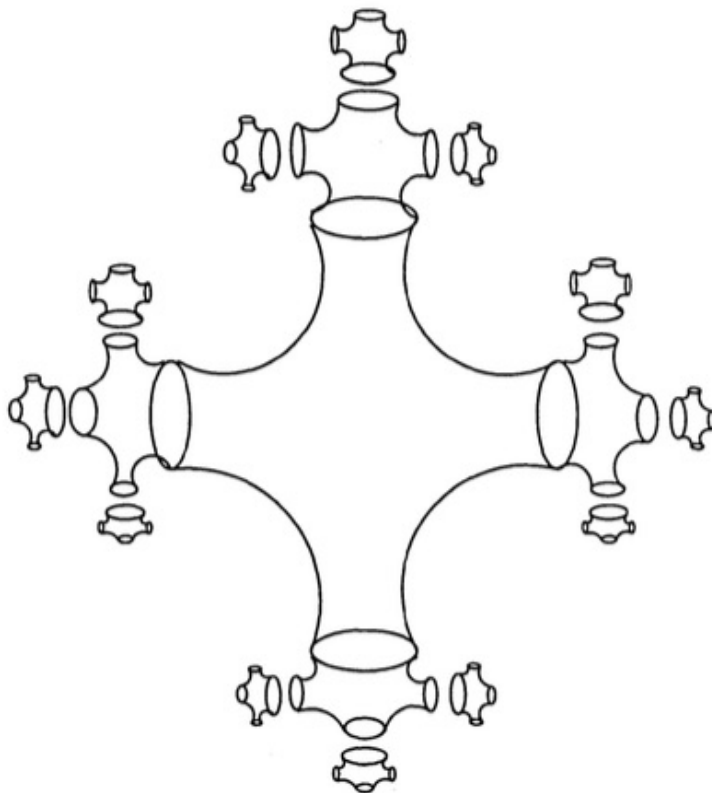
14

Figure 4: Fundamental domains for the action of Γ on $\mathbf{H}^3$.

In [37] and [36], Manin proposed to interpret the tangle of bounded geodesics inside the hyperbolic handlebody $\mathcal{H}_\Gamma$ as a model for the missing "closed fiber at infinity" in Arakelov geometry. This interpretation was based on the calculation of the Arakelov Green function [36], and the analogy with the theory of Mumford curves [43] and the computations of [35] for p-adic Schottky groups. The results of [36] and their holographic interpretation in [40], as well as the parallel theory of Mumford curves and periods of p-adic Schottky groups, will form the basis for our development of a p-adic and adelic form of the AdS$_{+1}$/CFT correspondence. The interpretation of the tangle of bounded geodesics in $\mathcal{H}_\Gamma$ as "closed fiber at infinity" of Arakelov geometry was further enriched with a cohomological interpretation in [18] (see also [19], [20] for the p-adic counterpart).

2.5   Bruhat–Tits trees, p-adic Schottky groups, and Mumford curves

The theory of Schottky uniformization of Riemann surfaces as conformal boundaries of hyperbolic handlebodies has a non-archimedean parallel in the theory of Mumford curves, uniformized by p-adic Schottky groups, seen as the boundary at infinity of a quotient of a Bruhat–Tits tree.

Some basic facts regarding the geometry of the Bruhat–Tits tree T_p of $\mathbb{Q}_p$ have been recalled in §2.2. More generally, the geometry we consider here applies to any finite extension $\mathbf{k}$ of the p-adic field $\mathbb{Q}_p$. By identifying $(\mathcal{O}_{\mathbb{Q}_p}/\mathfrak{m}^r) \otimes \mathcal{O}_\mathbf{k} = \mathcal{O}_\mathbf{k}/\mathfrak{m}^{re_\mathbf{k}}$, where $e_\mathbf{k}$ is the ramification index of $\mathbf{k}$ over $\mathbb{Q}_p$, we see that the Bruhat–Tits tree $T_\mathbf{k}$ for a finite extension $\mathbf{k}$ of $\mathbb{Q}_p$ is obtained from the Bruhat–Tits tree of $\mathbb{Q}_p$ by adding $e_\mathbf{k} - 1$ new vertices in each edge of $T_{\mathbb{Q}_p}$ and increasing the valence of all vertices to $p^f + 1$, where $f = [\mathbf{k} : \mathbb{Q}_p]/e_\mathbf{k}$, the degree of the extension normalized by the ramification index.

Let $\mathcal{O}_\mathbf{k}$ denote the ring of integers of $\mathbf{k}$ and $\mathfrak{m} \subset \mathcal{O}_\mathbf{k}$ the maximal ideal, so that the residue field $\mathcal{O}_\mathbf{k}/\mathfrak{m} = \mathbb{F}_q$ is a finite field with $q = p^r$ for some $r \in \mathbb{N}$. The set of vertices $V(T_\mathbf{k})$ of the Bruhat–Tits tree $T_\mathbf{k}$ of $\mathbf{k}$ is the set of equivalence classes of free rank two $\mathcal{O}_\mathbf{k}$-modules, under the equivalence $M_1 \sim M_2$ if $M_1 = \lambda M_2$, for some $\lambda \in \mathbf{k}^*$. For a pair of such modules with $M_2 \subset M_1$, one can define a distance function $d(M_1, M_2) = |l - k|$, where $M_1/M_2 = \mathcal{O}_\mathbf{k}/\mathfrak{m}^l \oplus \mathcal{O}_\mathbf{k}/\mathfrak{m}^k$. This distance is independent of representatives in the equivalence relation. There is an edge in $E(T_\mathbf{k})$ connecting two vertices in $V(T_\mathbf{k})$ whenever the corresponding classes of modules have distance one. The resulting tree $T_\mathbf{k}$ is an infinite homogeneous tree with vertices of valence $q + 1$, where $q = \#\mathcal{O}_\mathbf{k}/\mathfrak{m}$ is the cardinality of the residue field. The boundary at infinity of the Bruhat–Tits tree is identified with $\mathrm{P}^1(\mathbf{k})$. One can think of the Bruhat–Tits tree as a network, with a copy of the finite field $\mathbb{F}_q$ (or better of the projective line $\mathrm{P}^1(\mathbb{F}_q)$) associated to each vertex: this will be the guiding viewpoint in our approach to non-archimedean tensor networks.

The reader should beware that there is an unavoidable clash of notation: q is the standard notation for the modular parameter of an elliptic curve, but is also used to denote a prime power $q = p^r$ in the context of finite fields or extensions of the p-adics. While both uses will be made in this paper, particularly in this section and in §6.2, we prefer not to deviate from standard usage; it should be apparent from context which is intended, and hopefully no confusion should arise.

There is an action of $\mathrm{PGL}(2, \mathbf{k})$ on the set of vertices $V(T_\mathbf{k})$ that preserves the distance, hence it acts as isometries of the tree $T_\mathbf{k}$. A p-adic Schottky group is a purely loxodromic finitely generated torsion free subgroup of $\mathrm{PGL}(2, \mathbf{k})$. The Schottky group Γ is isomorphic to a free group on g-generators, with g the rank of Γ.

In this p-adic setting the loxodromic condition means that every nontrivial element γ in Γ has two fixed points $z_\gamma^\pm$ on the boundary $\mathrm{P}^1(\mathbf{k})$. Equivalently, an element γ is loxodromic if the two eigenvalues have different p-adic valuation. The closure of the set of fixed points $z_\gamma^\pm$, or equivalently the set of accumulation points of the action of Γ on $T_\mathbf{k} \cup \mathrm{P}^1(\mathbf{k})$ is the limit set Λ_Γ of the Schottky group Γ. The complement $\mathrm{P}^1(\mathbf{k}) \setminus \Lambda_\Gamma = \Omega_\Gamma(\mathbf{k})$ is the domain of discontinuity of the action of Γ on the boundary.

There is a unique geodesic ℓ_γ in $T_\mathbf{k}$ with endpoints $\{z_\gamma^-, z_\gamma^+\}$, the *axis* of a loxodromic element γ. The subgroup $\gamma^\mathbb{Z}$ acts on $T_\mathbf{k}$ by translations along ℓ_γ. There is a smallest subtree $T_\Gamma \subset T_\mathbf{k}$ that contains all the axes ℓ_γ of all the nontrivial elements $\gamma \in \Gamma$. The boundary at infinity of the subtree T_Γ is the limit set Λ_Γ.

T_Γ is the non-archimedean analog of the geodesic hull of the limit set of a Schottky group in $\mathbf{H}^3$.

The quotient $X_\Gamma(\mathbf{k}) = \Omega_\Gamma(\mathbf{k})/\Gamma$ is a Mumford curve with its p-adic Schottky uniformization, [43]. The quotient $T_\mathbf{k}/\Gamma$ consists of a finite graph T_Γ/Γ with infinite trees appended at the vertices of T_Γ/Γ, so that the boundary at infinity of the graph $T_\mathbf{k}/\Gamma$ is the Mumford curve $X_\Gamma(\mathbf{k})$. The finite graph $G_\mathbf{k} = T_\Gamma/\Gamma$ is the dual graph of the special fiber X_q (a curve over $\mathbb{F}_q$ which consists of a collection of $\mathrm{P}^1(\mathbb{F}_q)$ at each vertex of $G_\mathbf{k}$, connected along the edges). A family of finite graphs $G_{\mathbf{k},n}$, for $n \in \mathbb{N}$, is obtained by considering neighborhoods $T_{\Gamma,n}$ of T_Γ inside $T_\mathbf{k}$ consisting of T_Γ together with all vertices in $T_\mathbf{k}$ that are at a distance at most n from some vertex in T_Γ and the edges between them (these trees are preserved by the action of Γ), and taking the quotients $G_{\mathbf{k},n} = T_{\Gamma,n}/\Gamma$. The endpoints (valence one vertices) in $G_{\mathbf{k},n}$ correspond to the $\mathbb{F}_{q^n}$ points in the special fiber, $X_q(\mathbb{F}_{q^n})$, see [37]. One sees in this way, geometrically, how the $\mathbf{k}$-points in the Mumford curve $X_\Gamma(\mathbf{k})$ are obtained as limits, going along the infinite ends of the graph $T_\mathbf{k}/\Gamma$, which correspond to successively considering points of X_q over field extensions $\mathbb{F}_{q^n}$. Conversely, one can view the process of going into the tree from its boundary $X_\Gamma(\mathbf{k})$ towards the graph $G_\mathbf{k}$ in the middle of $T_\mathbf{k}/\Gamma$ as applying reductions to $\mathbb{F}_{q^n}$. We will see later in the paper how this process should be thought of physically as a form of renormalization. The finite graph $G_\mathbf{k} = T_\Gamma/\Gamma$ is the non-archimedean analog of the convex core $\mathcal{C}_\Gamma$ of the hyperbolic handlebody $\mathcal{H}_\Gamma$, while the infinite graph $T_\mathbf{k}/\Gamma$ is the non-archimedean analog of $\mathcal{H}_\Gamma$ itself, with the Mumford curve $X_\Gamma(\mathbf{k})$ replacing the Riemann surface $X_\Gamma = X_\Gamma(\mathbb{C})$ as the conformal boundary at infinity of $T_\mathbf{k}/\Gamma$.

Geodesics in the bulk space $T_\mathbf{k}/\Gamma$ correspond to images in the quotient of infinite paths without backtracking in the tree $T_\mathbf{k}$, with endpoints at infinity on $\mathrm{P}^1(\mathbf{k})$. Again, one can subdivide these in several cases. When the endpoints are the attractive and repelling fixed points $z_\gamma^\pm$ of some element $\gamma \in \Gamma$, the path in $T_\mathbf{k}/\Gamma$ is a closed loop in the finite graph $G_\mathbf{k}$. If the endpoints are both in Λ_Γ but not the fixed points of the same group element, then the geodesic is an finite path in $G_\mathbf{k}$ that is not a closed loop (but which winds around several closed loops in $G_\mathbf{k}$ without a fixed periodicity). If at least one of the endpoints is in $\Omega_\Gamma(\mathbf{k})$ then the path in $T_\mathbf{k}/\Gamma$ eventually (for either $t \to +\infty$ or $t \to -\infty$) leaves the finite graph $G_\mathbf{k}$ and wonders off along one of the attached infinite trees towards the boundary $X_\Gamma(\mathbf{k})$ at infinity. We still refer to these cases as closed, bounded, and unbounded geodesics, as in the archimedean case. We refer the reader to [25], [39], [43], [47] for a more detailed account of the geometry of Mumford curves.

3   Tensor networks

Motivated by the idea that the Bruhat–Tits tree T_p is a discrete (while still geometric) analogue of anti-de Sitter space, we will use this section to consider some relations between tensor networks that have been considered in the literature and the tree. One might imagine that many such relations can be drawn, and

we have made no effort to be exhaustive; indeed, a primary aim in writing this paper is to bring the p-adic geometry to the attention of researchers working on tensor-network approaches to holography, who (we hope) will find it both interesting and useful.

Throughout this section the basic Hilbert spaces in the bulk and the boundary will be those of finite dimensional qudits and the primary object of study will be the entanglement structure. In §4, the finite dimensional Hilbert spaces are replaced with those of a field theory valued in $\mathbb{R}$ or $\mathbb{C}$. We will find many aspects of holography hold in this field theoretic model and provide evidence for an exact correspondence. This connection puts the tensor network models of holography on a more equal footing with dynamical models, since both are defined from the same discrete spacetime.

We will focus our attention on the networks used by Pastawski, Yoshida, Harlow, and Preskill [45], (or "HaPPY"), in their construction of holographic quantum error-correcting codes. Such codes are easy to describe and admit many variations; in the simplest case, they are associated to a regular hyperbolic tiling of the plane. We will refer to such tilings by their *Schläfli symbol;* the notation $\{s, n\}$ refers to a tiling in which n regular polygons, each with s sides, meet at every vertex. A simple calculation shows that the tiling is hyperbolic whenever

$$n > \frac{2s}{s-2}. \tag{3.1}$$

For instance, if pentagons are used, $n = 4$ is the smallest possible choice ($n = 3$ would give the dodecahedron). If the tiles are heptagons or larger, any $n \geq 3$ gives a hyperbolic tiling.

Due to constraints of space, we will not fully review the HaPPY construction here; for details, the reader is referred to the original paper. The key point is that each tile carries a *perfect tensor*, which has an even number of indices, each of which refers to a qudit Hilbert space of fixed size. Such tensors are characterized by the property that any partition of the indices into two equal sets yields a maximally entangled state; we review perfect tensors in more detail, and construct a family of them associated to finite fields, in §3.1. Due to the appearance of finite fields in the construction of the tree, we feel this is the most natural family of tensors to consider.

The gist of our argument is that the natural "geometric" setting of a HaPPY tensor network (for certain uniform tilings) is the Bruhat–Tits tree corresponding to a prime p. We are motivated in this argument not only by the algebraic similarity between the constructions of T_p and AdS_3, but also by the fact that field-theoretic models of holography can be defined on the tree which exhibit it as the natural discrete setting for the AdS/CFT correspondence. In particular, the Bruhat–Tits tree with all edges of equal length can be thought of as a discrete analog of (empty) Euclidean AdS_3, and we conjecture that it is dual to the vacuum of the CFT living on $\mathbb{Q}_p$. It is therefore logical to guess that HaPPY tensor networks naturally encode information about the entanglement structure of the conformal field theories living at the finite places, and not about the CFT living at the Archimedean place.

The precise connection we identify is that, at least for certain choices, the tiling used in HaPPY's code (when thought of as a graph) has a spanning tree that is a Bruhat–Tits tree. In some sense, therefore, the tree represents the union of as many geodesics as can be marked on the tiling without creating closed paths in the bulk.

In HaPPY's original paper, a "greedy algorithm" (related to reconstruction of the quantum state input at the bulk or "logical" qubits of the code) is used to define a region of the bulk, the perimeter of which is then called a "geodesic." We will show in §3.4 that tree geodesics can be understood to correspond to these "greedy" geodesics for the $\{5, p+2\}$ tilings.

An analogue of the Ryu-Takayanagi formula holds for these codes, essentially because the length of the geodesic counts the number of bonds (contracted tensor indices) that cut across it, and—due to the properties of perfect tensors—each contributes a constant amount (the logarithm of the qudit dimension) to the entanglement entropy. For us, it will be crucial to note that the length of a (unique boundary anchored) tree geodesic is related to the p-adic size of the boundary region it defines. We will elaborate on this in §5; for now, we will simply remark on a few features of the formula that we will need in this section.

At the Archimedean place, entanglement entropy measures the entanglement between the degrees of freedom living on a spatial domain A of a QFT and those living on the complement A^c. In AdS_3, the domain A is usually taken to be an interval, or a collection of intervals. The finite place analogue of an interval is just an open ball (as defined in §2.1); the notion of "codimension" is counterintuitive in the p-adic setting! One can see that there is no topological difference between (for instance) an open subset of the unit circle, which would be an interval in the normal case, and a generic open subset.

If the Ryu-Takayanagi formula holds, the entanglement entropy between A and A^c is given by the length of the unique geodesic $\gamma\left(x_A, y_A\right)$ in the Bruhat–Tits tree connecting boundary points x_A and y_A,

$$S_{\mathrm{EE}}(A) = \# \cdot \text{length}\left(\gamma\left(x_A, y_A\right)\right). \tag{3.2}$$

Just as in the case of AdS_3, entanglement entropy is a logarithmically divergent quantity. The divergence arises because if x_A and y_A are on the boundary, the number of legs on the geodesic is infinite. To regularize this divergence, we introduce a cutoff ϵ_p such that the length of the geodesic is

$$\text{length}\left(\gamma\left(x_A, y_A\right)\right) = 2\log_p \left| \frac{x_A - y_A}{\epsilon_p} \right|_p, \tag{3.3}$$

with $|\cdot|_p$ the p-adic norm. (For details about this, see §5.1.) This gives the entanglement entropy between

A and its complement in $\mathbb{Q}_p$ as[1]

$$S_{\text{EE}}(A) = \# \log_p \left| \frac{x_A - y_A}{\epsilon_p} \right|_p . \tag{3.4}$$

The proportionality constant will be left undetermined for now.

3.1 Perfect tensors and quantum error-correcting codes from finite fields

Our goal in this subsection is to recall some features of quantum error-correcting codes associated to $2n$-index perfect tensors, as used by Pastawski, Yoshida, Harlow, and Preskill [45]. We will review the three-qutrit code and associated four-index perfect tensor that they construct, and then show how this is the case $q = 3$ of a family of perfect tensors associated to powers $q = p^m$ of odd primes. While the corresponding quantum error-correcting codes are not new [28], our goal is to highlight the properties of these particular codes that make them relevant to p-adic holography. In particular, as we recalled in §2.5, each vertex of the Bruhat–Tits tree for a degree-n unramified extension k of $\mathbb{Q}_p$ is marked with a copy of the residue field $\mathbb{F}_{p^n}$. As such, finite fields appear as important ingredients both in the construction of holographic tensor networks and in the algebraic setting of the Bruhat–Tits tree. We feel that the codes discussed here are natural candidates to consider in connecting p-adic geometry to tensor network models, although of course this choice is not inevitable and any code with the right properties will define a holographic code.

3.1.1 The three-qutrit code

In their paper, Pastawski *et al* consider the following quantum error-correcting code, which encodes a one-qutrit logical Hilbert space in a three-qutrit physical Hilbert space:

$$|0\rangle \mapsto |000\rangle + |111\rangle + |222\rangle$$
$$|1\rangle \mapsto |012\rangle + |120\rangle + |201\rangle$$
$$|2\rangle \mapsto |021\rangle + |102\rangle + |210\rangle .$$

The encoded data is protected against erasure of any single qutrit. If we represent the state by a tensor,

$$|a\rangle \mapsto T_{abcd} |bcd\rangle ,$$

---

[1]For the length of the geodesic between x_A and y_A to warrant the interpretation of entanglement entropy, it must be the case that the tensor network bonds cutting across it, when extended all the way to the boundary, connect between A and A^c. This can be done and is explained in §3.4.

then T_{abcd} is perfect in the sense of Pastawski *et al*, and defines a perfect state:

$$|\psi\rangle = T_{abcd} |abcd\rangle.$$

(Throughout, we use Einstein's summation convention.) To recall, a tensor with $2n$ indices, each representing a qudit Hilbert space of any chosen fixed size, is perfect when it satisfies any of the following equivalent conditions:

- Given any partition of the indices into two disjoint collections $A \sqcup B$, where $|A| \leq |B|$, the tensor defines an injection of Hilbert spaces $\mathcal{H}_A \hookrightarrow \mathcal{H}_B$: a linear map that is a unitary isomorphism of its domain with its image (carrying the subspace norm).

- The corresponding perfect state is maximally entangled between any tensor factors $\mathcal{H}_{A,B}$ of equal size (each consisting of n qudits). That is, after tracing out n of the $2n$ qudits, the remaining n-qudit density matrix is proportional to the identity operator.

It is straightforward to check that the above tensor T_{abcd} is an $n = 2$ perfect tensor on qutrits. To rephrase the way it is constructed so as to make its generalization to larger codes more apparent, we notice that the particular states that appear in the encoding of a basis state $|a\rangle$ are lines of slope a in $\mathbb{F}_3^2$: if the three qudits are labeled by an element x of F_3, then the states are of the form $\otimes_x |f(x)\rangle$, where $f(x) = ax + b$, and we sum over the three possible choices of $b \in \mathbb{F}_3$. The result is a perfect tensor because a line is determined either by two of its points, or by one point and knowledge of the slope; conversely, given any two points, or any one point and one slope, exactly one corresponding line exists.

3.1.2 Perfect polynomial codes

We would like to generalize this to a family of perfect tensors in which the qudit Hilbert spaces are of size $q = p^m$, so that a basis can be labelled by the elements of $\mathbb{F}_q$. An obvious guess is to associate a function or collection of functions $f_a : \mathbb{F}_q \to \mathbb{F}_q$ to each logical basis state $|a\rangle$, generalizing the collection of lines $f_a(x) = ax + b$ that were used when $q = 3$. These functions should have the property that knowledge of some number of evaluations of f_a will uniquely specify a, whereas knowing any smaller number of evaluations will give no information about a whatsoever. The encoded states will then take the form $\sum_b (\otimes_x |f_a(x)\rangle)$, for some collection of x's in $\mathbb{F}_q$. Here b stands for a collection of numbers parameterizing the set of functions f_a.

The simplest choice of such a class of functions are polynomials of fixed degree d:

$$f_a(x) = ax^d + b_{d-1}x^{d-1} + \cdots + b_1 x + b_0.$$

21

Over the real numbers, $d + 1$ points determine such a polynomial. Over finite fields, one must be a little careful—by Fermat's little theorem,

$$x^q - x = 0 \ \forall x \in \mathbb{F}_q.$$

As such, if $d \geq q$, we can't determine a polynomial uniquely by its evaluations—after all, there are at most q possible evaluations over a finite field! However, polynomials of degree $d < q$ can be recovered uniquely; in fact, every function from $\mathbb{F}_q$ to $\mathbb{F}_q$ is a polynomial function, uniquely represented by a polynomial of degree $d < q$ (there are exactly q^2 elements of each collection).

However, if we choose d too large, the resulting code will not have error-correcting properties: we will need almost all of the physical qudits to recover the logical one. We know that for codes obtained from $2n$-index perfect tensors, one logical qudit is encoded in $2n - 1$ physical qudits, and is recoverable from any n of them. This is sometimes called a $[[2n - 1, 1, n]]_q$ code. For polynomial codes, we must have $2n - 1 \leq q$ (since there are at most q possible evaluations of the code function), and furthermore $n = d + 1$. Thus, the largest possible perfect tensor we can obtain from this class of codes has $p + 1$ indices, corresponding to the $[[q, 1, (q+1)/2]]_q$ code; the polynomials used in making this code are of degree $d = (q-1)/2$. Recall that we are assuming $p \neq 2$ everywhere; $q = 3$ recovers the linear qutrit code that we discussed above.

To be concrete, when $q = 5$, the code takes the following form:

$$|a\rangle \mapsto \sum_{b_0, b_1 \in \mathbb{F}_5} |b_0, b_0 + b_1 + a, b_0 + 2b_1 + 4a, b_0 + 3b_1 + 4a, b_0 + 4b_1 + a\rangle.$$

The numbers that appear are just x as the coefficient of b_0 and x^2 as the coefficient of a. This encoded state already contains 25 basis states, and the perfect state $|\psi_5\rangle$ constructed from this tensor is a combination of $5^3 = 125$ basis states.

These $p+1$-index perfect tensors seem like logical candidates to use in constructing a family of quantum codes associated to Bruhat–Tits trees. In particular, they are naturally associated to the data of a finite field $\mathbb{F}_q$, which appears at each vertex of the tree; moreover, they have $q + 1$ qudit indices, which agrees with the valence of the tree.

However, the exact way to combine these ingredients remains a little unclear. In particular, since paths in the tree correspond to geodesics in the p-adic hyperbolic space, it seems more natural to think of the legs of the tree as *cutting across* contractions of tensor indices, rather than representing them. We expand on this idea in the section that follows.

3.2 Bruhat–Tits trees and tensor networks

We now investigate the connection between Bruhat–Tits trees and tensor networks. The gist of this section is that, while the tree corresponds to "geometry," the tree alone cannot define a tensor-network topology in the most naive way (tensors at vertices with indices contracted along edges). This is because, in typical tensor-network models of holography, the Ryu-Takayanagi formula holds because each unit distance along a geodesic corresponds to a bond (i.e., contracted tensor index) which is "cut" by the path and contributes a fixed amount (the logarithm of the dimension of the qudit Hilbert space) to the entanglement entropy. Since the paths in the tree correspond to geodesics in the bulk, one cannot hope to connect the tree to HaPPY's holographic code without adding tensors in such a way that their indices are contracted *across* the edges of the tree.

The extra structure we need to account for the network can be as simple as grouping the vertices of the tree in some fashion, associating bulk indices to the groups, and demanding perfect tensor structure, as we now explain.

> **A basic set of rules for constructing entanglement:** Group the vertices in the tree in some way; to each grouping we associate one or more bulk vertices. If two groupings share two tree vertices, then there is a tensor network bond connecting the bulk vertices of the groupings. The resulting tensor network should be composed of perfect tensors. This constructs a tensor network mapping between the boundary and the bulk.

It is not clear what the most general rules for associating the tensor vertices to the tree vertices should be. In particular, we are not demanding planarity (the Bruhat–Tits tree has no intrinsic planar structure), so the resulting network could be quite complicated, or even pathological. In order for the nice properties of a bulk-boundary tensor network to hold additional criteria should likely be imposed. We leave the general form of these criteria for future work; in the following, we focus on one specific set of rules that works.

3.3 Bruhat–Tits spanning trees of regular HaPPY tilings

Although the most general set of rules for assigning tensors is unclear, HaPPY tensor networks of uniform tiling can easily be constructed from the minimal proposal above with the addition of a few simple rules. These extra rules introduce planarity, so that the Bruhat–Tits tree becomes the spanning tree of the graph consisting of the edges of the HaPPY tensor network tiles. For $q > 3$, we can construct a HaPPY tensor network associated to a $[[q, 1, (q + 1)/2]]_q$ code by grouping the vertices of the tree into sets of q, corresponding to tessellation tiles, and adding one bulk vertex to each tile. These tiles are organized into

"alleyways;" each tile consists of vertices connected by a geodesic for tiles that are the starting points of alleyways, or of vertices living on two geodesics for tiles along the alleyway (see Fig. 5). The edges of each tile consist of either $q-1$ or $q-2$ segments coming from the geodesics, and one or two fictitious segments (the dotted lines in Fig. 5) respectively, that we draw only to keep track of which tree vertices have been grouped. Furthermore, each vertex connects to exactly one dashed edge. Since the tree has valence $q+1$, the HaPPY tensor network tiling has $q+2$ tiles meeting at each vertex.

The description above works for $q > 3$. The case $q = 2$ is special and can be obtained from the $[[5, 1, 3]]_2$ code; this is the case depicted in Fig. 5. In fact, any size polygon could be used; the only real constraint is that the tiling be hyperbolic of the form $\{n, q+2\}$, with q a prime power. The pathologies of low primes come from the difficulty in demanding the tiling be hyperbolic and requiring perfect tensors; for instance, the $p = 2$ case would require a 3 index perfect tensor, but all perfect tensors have an even number of indices by construction.

In this picture of tiles, the tensor network bonds can be thought of as cutting across the edges of the tiles. Indeed, because of planarity, each edge can be associated with the tensor network bond of its vertices, precisely reproducing the HaPPY construction for uniform tilings of the hyperbolic plane.[2]

An interesting feature of our construction is that it introduces a peculiar notion of distance on the boundary, in that points $x, y, \in \mathbb{Q}_p$ that are that are far apart (in terms of the norm $|x - y|_p$) can belong to the same tile, or to neighboring tiles, so they can be "close in entanglement"; this is a concrete manifestation of the dissociation between entanglement and geometry inherently present in our model.

3.3.1 Explicit tree-to-tessellation mapping

We now explicitly construct an identification between Bruhat–Tits trees and a HaPPY tensor network of uniform tiling. The end goal is to show that a planar graph of uniform vertex degree v admits a spanning tree of uniform vertex degree $v - 1$. Although both the degree of the tree and the size of the tile are constrained by the quantum error correcting code, for the sake of generality we will work with n-gonal tiles, $n \geq 5$, and trees of valence k, $k \geq 3$. The algorithm constructing the mapping proceeds by starting with one n-gonal tile, then builds regions of tiles moving radially outward. Each region is built counterclockwise.[3]

The purpose of this algorithm is to build a graph of dashed and solid edges such that every vertex has degree $k + 1$ and exactly one dashed edge connecting to it. The HaPPY tensor network tiling is given by the solid and dashed edges, and the tree is given by the solid edges, as in Fig. 5. The steps of the algorithm are as follows (see also Fig. 6 for a pictorial representation):

---

[2]We should always remember, however, that in our construction, unlike in [45], bulk indices and tensor network connections are fundamentally associated to groups of tree vertices, and not to the geometric elements of a tile.

[3]There are, of course, many variations of this algorithm that work; here we only exhibit one of them. For the purposes of constructing the mapping, it does not matter which variation we use.
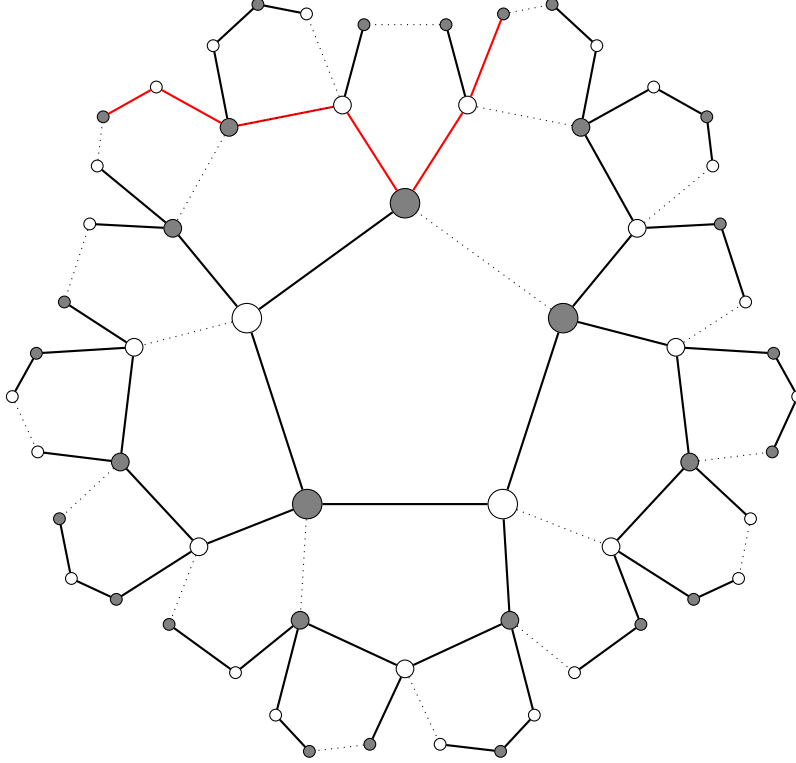
Figure 5: Mapping between a $p = 2$ Bruhat–Tits tree and the regular hyperbolic tiling $\{5, 4\}$. The first three regions constructed by the algorithm are shown. The red geodesic separates the causal wedge for the boundary region on which the geodesic ends from its complement in the tree. Since this is $p = 2$, the number of edges in a tile is different than our standard choice in the arbitrary q case.

1. Start with an n-gonal tile with one edge dashed and $n - 1$ solid edges. This is region $r = 1$. The left vertex of the dashed line is the current vertex.

2. To construct region $r + 1$, for the current vertex, add an edge e_f extending outward, then go counterclockwise around the tile being created, breaking off the edges shared with region r as soon as a vertex with degree less than $k + 1$ is encountered. Call the first new edge after breaking off e_n. If either e_f or e_n are constrained (by the condition that in the graph we want to obtain each vertex has degree $k + 1$ and precisely one dashed edge connecting to it) to be dashed, make them dashed, otherwise they are solid. If neither e_f nor e_n are dashed, make the "farthest" edge (call it e_l) dashed; otherwise, leave it as a solid edge. e_l is chosen so that its distance to the existing graph is as large as possible, and so equal on both sides if possible; if the number of new edges is even, so that this prescription is ambiguous, the choice closer to e_f is taken.

3. Move counterclockwise to the next vertex on the boundary of the current region, skipping any vertices of degree $k + 1$. This new vertex becomes the current vertex.

4. Repeat the step above until we have built an edge e_f on all vertices of region r that have degree less than $k + 1$. This completes region $r + 1$.

5. To start on the next region, set the current vertex to be the left vertex of the dashed line on the first $r + 1$ tile that we built, then go to step 2 above.

We now show why the algorithm works:

- By induction, there can be no neighboring vertices of degree greater than two on the boundary at any step, except when building a tile on the next-to-last edge of a tile from the previous region, in which case a vertex of degree 3 neighbors a vertex of some degree. This is because if the boundary has no neighboring vertices of degree $k + 1$, any tile we add shares with the boundary of the previously constructed tiles at most two edges, so (since $n \geq 5$) it will have at least three free edges, adding at least two vertices of degree 2 between the vertices to which it connects.

- From the previous point, when constructing any tile, the vertices to which e_f and e_n connect cannot both have degree k before adding e_f and e_n, so either e_f or e_n can be made solid.

- If e_f and e_n are not dashed, then e_l only connects to two solid edges, so it can be made dashed.

- By the above, each new tile we add introduces exactly one dashed edge, so the graph of solid edges remains a tree at all steps.

This completes the proof.

3.4   Bulk wedge reconstruction

In this subsection we discuss how bulk reconstruction, in the sense of [45], functions for our proposal. Although the construction in §3.3 replicates the tensor network tiling of [45], there are some differences of interpretation.

The algorithm outlined in Pastawski *et al.*'s paper prescribes that, starting with a given boundary region, one should add tiles one by one if the bulk qubits they carry can be reconstructed from the known data; i.e., if one knows (or can reconstruct) a majority of the edge qubits on the tile. When no further tiles can be added in this manner, the reconstruction is complete, and the boundary of the region is the "greedy geodesic."

In our case, for a given drawing of the tree, the first step to reconstructing a boundary open set $|x_A - y_A|_p$ is to identify a geodesic $\mathcal{G}$ that separates the causal wedge for the boundary region on which $\mathcal{G}$ ends from its complement in the tree. This is nontrivial, because due to the non-planarity of the tree, paths that end on the ball corresponding to the endpoints of the geodesic can be drawn outside the wedge. A $\mathcal{G}$ with the
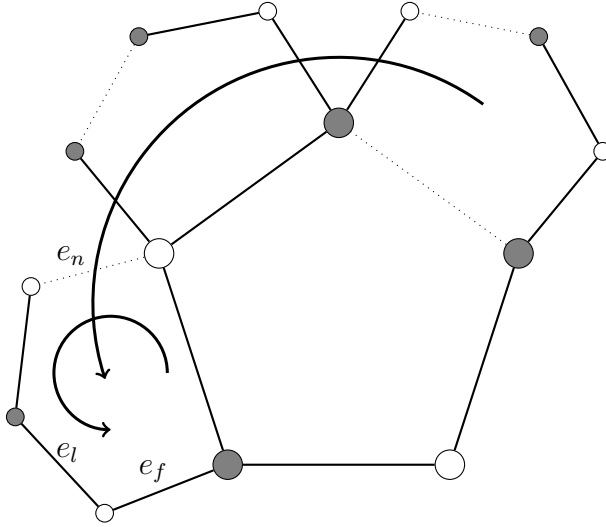
Figure 6: Mapping between a $p = 2$ Bruhat–Tits tree and a pentagonal HaPPY tiling, after the third tile of the second region has been built. Edge e_n is constrained to be dashed, so edges e_f and e_l are solid. The arrows represent the direction in which the algorithm constructs regions and tiles.

desired property is a geodesic from which only one path leaves into the complement of the wedge; such an example is drawn in Fig. 5 in red. Given a choice of planar structure, there is a unique "outermost" separating geodesic associated to each open set. Once a separating geodesic has been identified, we can assign x_A and y_A to its endpoints, the inside of the ball to the tree inside the wedge, and the complement of the ball to the complement of the wedge in the tree.

For the tilings $\{5, n\}$, it is straightforward to see that the greedy geodesic for a boundary open ball coincides with the tree geodesic $\mathcal{G}$ that forms the "boundary" of that open ball in the chosen planar structure. The alleyways in the diagram are sequences of tiles joined along dashed lines, such that fewer than half of the edges on each tile are exposed to either side; therefore, each alleyway forms a "firebreak," which the greedy algorithm cannot jump across. If none of the dashed edges are known, none of the tiles in the alleyway can be reconstructed. Therefore, starting at a boundary open set, the greedy algorithm propagates up the alleyways whose ends lie inside the region, and fills out the region marked off by the tree geodesic. It cannot stop before the region is filled, since by construction each tile neighbors at least three tiles that are further away from the center than the tile itself is.

When the tiles are larger than pentagons, a difficulty arises when one is building tiles for which two edges touch the previous part of the picture: one may be forced (by valence requirements) to build a dashed edge at e_n or e_f, while another dashed edge exists in the previously built part, a distance of only one away. An instance where this occurs (although, of course, it causes no problems for pentagonal tiles)

can be seen at the bottom right corner of Fig. 5. This constructs an alley that could be jumped by the greedy algorithm.

A simple fix for this problem would be to simply use a pentagon whenever this situation arises, resulting in a nonuniform tiling where the alleyways still function as firebreaks. While this will produce a valid holographic code, it is not immediate that the tiling is even regular in this case.

Another option is, if we are willing, to alter the tiling near a specifically chosen geodesic, so that the problem does not arise for that particular wedge. We explain an algorithm to construct the tiling in this case. The idea is to construct two alleyways, with the sides with one edge per tile pointing towards the wedge. This separates the plane into two regions, that for the purposes of tile building don't talk to each other. Since the rules for building a tile from Sec. 3.3 are (almost) local, they have no information the global structure of the row being built. It is thus possible to use them to cover the two regions, moving "left" and "right" to create rows, and "up" and "down" to stack the rows. We give the explicit steps of the algorithm (see Fig. 7):

1. Build an alley of k-gons, by starting with a k-gon with one dashed edge (call this the root tile) and building the successive gons always on the dashed edges. For each k-gon except for the starting one, the number of solid edges on the two sides of the dashed edges should be 1 and $k-3$ respectively, with all 1's occurring on one side, and all $(k-3)$'s on the other.

2. Build a second alley of k-gons, starting on the solid edge of the root tile that neighbors the root's dashed edge on the side of 1's. For each k-gon except the starting one, the number of solid edges on the two sides of the dashed edges should be 1 and $k-3$ respectively, with all 1's facing the 1's of the first alley. The plane has now been split into two regions: wedge and complement.

3. To construct the tiling inside the wedge, start on some edge of the two central alleyways, and construct a tile using the rules from point 2 in the algorithm in Sec 3.3. Then move to the right, and construct new tiles rotating clockwise in the construction of each tile. To do the other side, start from the initial tile and move left, constructing tiles using the rules from point 2 in the algorithm while rotating counterclockwise. This fills a "row".

4. Once the "row" is complete, move to the row "above" it and repeat.

5. To construct the tiling of the complement of the wedge, run the two bullet points above, but having the clockwise and counter-clockwise rotations swapped, and moving "below" instead of "above".

This algorithm works because locally the construction is the same as the one in the algorithm of Sec 3.3. The individual tile building procedure does not depend on whether it is going around a finite region (as in
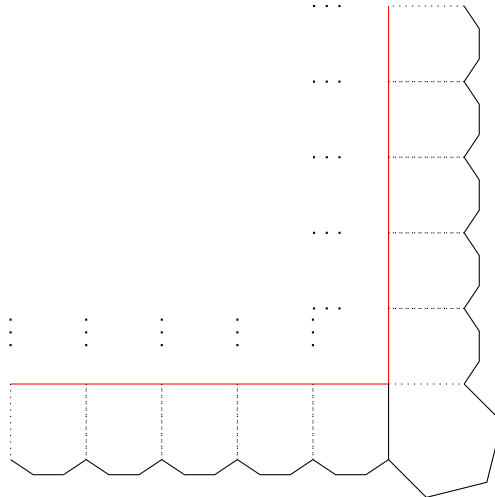
Figure 7: Mapping between the tree and tiling for reconstructing a chosen causal wedge. The two central alleys partition the plane into two regions: the causal wedge of the red geodesic and its complement. Tilings can be constructed to either side of the shown alley by building tiles via step 2 of the algorithm of Sec. 3.2.

Sec. 3.3), or along an infinite "row". And since inside the wedge more than half of each tile's neighbors are further away from the center than the tile is, the reconstruction covers the entire wedge.

While in the original HaPPY construction [45] one tensor network suffices to reconstruct the causal wedge associated to any boundary interval, in our case the tree identifies a certain collection of open sets on the boundary when pentagonal tiles are used (and, in one possible generalization to larger tiles, may even treat one boundary region as special). Even for pentagons, there may be many ways to draw the spanning tree on the same tiling. Moreover, the boundary tiles are not treated on an equal footing: they form the ends of shorter and longer alleyways. The longer the alleyway in which a boundary tile appears, the larger the first open set that includes it. One can think of these extra choices as follows: If one were to draw all possible greedy geodesics on the tiling, all edges would be marked, and there would be no information. Marking the geodesics with a subgraph is only useful when there is a unique path between pairs of boundary points, so that one knows "which way" to turn in order to recover the geodesic. This means that the marked subgraph should have no closed loops: that is, it should be a tree, and the spanning tree is (by definition) a largest possible subtree.

3.5 Entanglement bridges

By choosing a planar assignment of tensors, we have found the Bruhat-Tits tree as the spanning tree of this tiling. Although this choice was convenient, it may be somewhat arbitrary. One might ask for more exotic non-planar way of connecting the tree with tensors. Such a non-planar structure might obscure the

geometric interpretation, but it is expected that quantum gravity contains non-geometric states, so there is a sense in which at least small deviations from planarity should be physically acceptable. One simple example might be to connect two distant parts of the tree together through a non-planar tensor. If this can be done in a consistent way, one might interpret this non-planar defect a bridge of entanglement between two points of the tree. It would be interesting to investigate whether a configuration with defects or more complicated non-planar structures, can be understood in terms of the ER = EPR proposal [34].

Furthermore, the rules we have identified here still generically break symmetries of the tree, since a $\mathrm{PGL}(2, \mathbb{Q}_p)$ transformation need not preserve the grouping of vertices or the planar structure. One might hope to construct a tensor network associated to the tree with more minimal auxiliary structure, so that the full symmetry group of the p-adic bulk spacetime is manifest for the network as well; however, for the reasons outlined above, it is difficult to understand how to do this while making contact with tensor network proposals existing in the current literature.

4 p-adic conformal field theories and holography for scalar fields

In this section, we turn from tensor networks to genuine field theories defined on p-adic spacetimes: either in the bulk of the tree T_p (or possibly a quotient by a Schottky group) or on a p-adic algebraic curve at the boundary. We will find evidence for a rich holographic structure strongly reminiscent of ordinary AdS/CFT. The conformal theory on the fractal p-adic boundary is analogous to 1+1 dimensional field theory with a p-adic global conformal group; our principle example is the p-adic free boson which permits a Lagrangian description. In the bulk, semi-classical massive scalar fields defined on the lattice model naturally couple to operators on the conformal boundary in a way that allows for precise holographic reconstruction. One can also interpret the radial direction in the tree as a renormalization scale. These observations unite discrete analogs of AdS geometry, conformal symmetry, and renormalization in a holographic way.

4.1 Generalities of p-adic CFT, free bosons, and mode expansions

While non-archimedean conformal field theory has been considered in the literature from several different perspectives [42, 10, 59], it remains much less well-studied than ordinary two-dimensional CFT. Melzer [42] defines these theories in general by the existence of an operator product algebra, where all operators in the theory are primaries with the familiar transformation law under the global conformal group $\mathrm{SL}(2, \mathbb{Q}_p)$. Descendants are absent in Melzer's formulation because there is no analogue of the derivative operators ∂ and $\bar{\partial}$ acting on complex-valued functions over $\mathbb{Q}_p$ [42], and (correspondingly) no local conformal algebra.

In this formulation, the correlation function between two primary fields $\phi_m(x)$ and $\phi_n(y)$ inserted at

points x and y and having scaling dimensions Δ_n is given (after normalization) by

$$\langle \phi_m(x)\phi_n(y) \rangle = \frac{\delta_{m,n}}{|x-y|_p^{2\Delta_n}}. \tag{4.1}$$

(We will understand this formula holographically in what follows.) As in the archimedean case, as we take the points x and y to be close together (p-adically), we wish to expand the product as a sum of local field insertions: the operator product expansion. For two such primaries $\phi_m(x)$ and $\phi_n(y)$, there exists an $\epsilon > 0$ such that for $|x-y|_p < \epsilon$, the correlation function (perhaps with other primaries $\phi_{n_i}(x_i)$ inserted) is given by the expansion:

$$\langle \phi_m(x)\phi_n(y)\phi_{n_1}(x_1)\dots\phi_{n_i}(x_i) \rangle = \sum_r \tilde{C}_{mn}^r(x,y)\langle \phi_r(y)\phi_{n_1}(x_1)\dots\phi_{n_i}(x_i) \rangle, \tag{4.2}$$

where the sum runs over all primaries in the theory, and $\tilde{C}_{mn}^r(x,y)$ are real valued. This relation should hold whenever $|x-y|_p$ is smaller than the distances to the x_i's. Invariance under $SL(2,\mathbb{Q}_p)$ implies

$$\tilde{C}_{mn}^r(x,y) = C_{mn}^r |x-y|_p^{\Delta_r - \Delta_m - \Delta_m} \tag{4.3}$$

with constant OPE coefficients C_{mn}^r.

Theories defined in this way enjoy a number of special properties not true of their archimedean counterparts. They are automatically unitary since they possess no descendant fields. Additionally, because $\mathbb{Q}_p$ is an *ultrametric* field, all triangles are isosceles: for $x, y, z \in \mathbb{Q}_p$, from the p-adic norm we have

$$\text{If } |x-y|_p \neq |y-z|_p \text{ , then } |x-z|_p = \max\left\{|x-y|_p, |y-z|_p\right\}. \tag{4.4}$$

This fundamental property of the p-adic numbers implies that the three- and four-point functions are *exactly* determined by the conformal weights and OPE coefficients. In the case of the four-point function, after an $\mathrm{SL}(2, \mathbb{Q}_p)$ transformation which maps three points to $0, 1$, and ∞, the only free parameter (the cross ratio of the original points) must be contained in a ball in the neighborhood of one of the other points. Since the OPE is exact in each neighborhood, one can compute the three possible cases and determine the full four-point function.

In fact, all higher-point functions are constrained by global conformal symmetry alone; by contrast, the spectrum of OPE coefficients is less constrained than in familiar CFTs. A consistent model can be constructed using the structure constants of any unital commutative algebra, subject to one simple condition. These features may be of interest in the study of conformal field theory and conformal blocks, but we do not pursue that direction here; the interested reader is referred to [42].

Let us now step back and consider the p-adic theory from the perspective of quantizing a classical field theory described by a Lagrangian. Many familiar objects from the study of quantum fields over normal (archimedean) spacetime have direct analogues in the p-adic setting. For example, one frequently makes use of the idea of a *mode expansion* of a field on flat spacetime in terms of a special class of basis functions, the plane waves:

$$\phi(x) = \int_{\mathbb{R}} dx \, e^{ikx} \tilde{\phi}(k). \tag{4.5}$$

The functions e^{ikx} are eigenfunctions of momentum, or equivalently of translations. Mathematically, we can think of these as *additive characters* of $\mathbb{R}$: they are group homomorphisms $\chi : \mathbb{R} \to \mathbb{C}$, such that $\chi(x+y) = \chi(x)\chi(y)$.

The additive characters of the fields $\mathbb{Q}_p$ are also known: they take the form [56]

$$\chi_k(x) = e^{2\pi i \{kx\}}. \tag{4.6}$$

Here $k, x \in \mathbb{Q}_p$, and the normalization factor 2π is included for convenience (in keeping with the typical math conventions for Fourier transforms). The symbol $\{\cdot\} : \mathbb{Q}_p \to \mathbb{Q}$ denotes the *fractional part* of the p-adic number.[4] It is defined by truncating the decimal expansion to negative powers of the prime:

$$\left\{ \sum_{k=m}^{\infty} a_k p^k \right\} = \sum_{k=m}^{-1} a_k p^k, \tag{4.7}$$

where the right-hand side is interpreted as an ordinary rational number, understood to be zero when the range of the sum is empty (m is non-negative). Since a p-adic number and its fractional part differ (at least in a formal sense) by an integer, it makes sense that the complex exponential (4.6) should depend only on the fractional part of kx. (However, care should be taken: in general, it is not true for rational x that $e^{2\pi i x} = e^{2\pi i \{x\}_p}$! For instance, $0.1 = 1/10$ is a 3-adic integer.)

A wide class of scalar fields on $\mathbb{Q}_p$ can be expanded in a basis of the additive characters, just like a mode expansion in the archimedean setting:

$$\phi(x) = \int d\mu(k) \, e^{2\pi i \{kx\}} \, \tilde{\phi}(k). \tag{4.8}$$

Here $d\mu(k)$ is the Haar measure on $\mathbb{Q}_p$. The theory of the p-adic Fourier transform is developed in more detail in Appendix A.

Our principal example (and also by far the most well-studied instance) of a p-adic conformal field theory

---

[4]As with other notations referring to the p-adics, we will sometimes use the subscript $\{\cdot\}_p$ when it is necessary for emphasis or to make reference to a specific choice of prime.

is the free boson: a single (real or complex) scalar field on $\mathrm{P}^1(\mathbb{Q}_p)$ or another p-adic Riemann surface, with a massless quadratic action. This theory was of interest in the context of p-adic string theory, in which the worldsheet is a p-adic space, but the target space (and hence all physically observable quantities) are ordinary. Many results were derived in that literature, including the well-known Freund–Olson–Witten tachyon scattering amplitudes [24, 23, 11].

Our interpretation of the system in question will be somewhat different, as we will emphasize the holographic nature of the interplay between field theory defined on a Riemann surface (algebraic curve) and the study of its hyperbolic filling, a quotient of the Bruhat–Tits tree. (In the p-adic string literature, it was common to view the tree as playing the role of the "interior" of the worldsheet.) Many of our results will parallel aspects of the p-adic string, but we will view this theory as a CFT on $\mathrm{P}^1(\mathbb{Q}_p)$ without any reference to a target space.

The p-adic free boson is considered here because it permits a Lagrangian description in terms of the nonlocal Vladimirov derivative, $\partial_{(p)}$, which acts on complex- or real-valued fields of a p-adic coordinate. This derivative is defined by

$$\partial_{(p)}^n f(x) = \int_{\mathbb{Q}_p} \frac{f(x') - f(x)}{|x' - x|_p^{n+1}} dx'. \tag{4.9}$$

In the p-adic string literature, $\partial_{(p)}$ is also known as a normal derivative, for reasons that will become clear in the following sections. Intuitively, the formula is similar to Cauchy's representation of the n-th derivative of a function by a contour integral. A more detailed explanation of its properties is given in Appendix B. While the parameter n is often taken to be an integer, it may in principle assume any real value.

One can arrive at the following action either by "integrating out" the interior of the string worldsheet T_p as done in [58], or by hypothesis as the minimal "quadratic" action of a scalar over a p-adic coordinate[21]. The action for a single scalar is (setting the overall coupling to 1) [50, 60, 27]:

$$S_p[\phi] = -\int_{\mathbb{Q}_p} \phi(x)\partial_{(p)}\phi(x)dx. \tag{4.10}$$

where $\partial_{(p)}\phi(x)$ is the first Vladimirov derivative of the field ϕ. We take $\phi(x)$ to be a scalar representation of the conformal group (see [49] for discussion of representations of $\mathrm{SL}(2, \mathbb{Q}_p)$.) Under an element

$$g = \begin{pmatrix} a & b \\ c & d \end{pmatrix}$$

of the conformal group, where $a, b, c, d \in \mathbb{Q}_p$ and $ad - bc = 1$, quantities in the above expression transform

33

as

$$x \to \frac{ax + b}{cx + d}, \quad x' \to \frac{ax' + b}{cx' + d},$$

$$dx \to \frac{dx}{|cx + d|_p^2}, \quad dx' \to \frac{dx'}{|cx' + d|_p^2},$$

$$|x' - x|_p^{-2} \to |(cx' + d)(cx + d)|_p^2 |x' - x|_p^{-2}.$$

As in [42], a field $\phi_n(x)$ having conformal dimension Δ_n transforms as

$$\phi_n(x) \to \phi_n'\left(\frac{ax + b}{cx + d}\right) = |cx + d|_p^{-2\Delta_n} \phi_n(x) \tag{4.11}$$

under the p-adic conformal group. For the free boson $\phi(x)$, we claim $\Delta = 0$. With this one can see the derivative $\partial_{(p)}\phi(x)$ carries a weight $|cx + d|_p^{-2}$ and thus is a field of dimension 1. It should now be clear that the action $S_p[\phi]$ is invariant under the global conformal group.

Given the action $S_p[\phi]$, we can define the partition function in the usual way by integrating over configurations with measure $\mathcal{D}\phi$. As in the case of the p-adic string, because ϕ is a complex (and not p-adic) valued field, this integration measure is exactly the one that appears in ordinary field theory:

$$Z_p = \int \mathcal{D}\phi \, e^{-S_p[\phi]}. \tag{4.12}$$

As many authors have noted [50, 60, 46]:, this action and the partition function actually describe a free theory. This means the saddle point approximation to the partition function is exact, and it can be computed by Gaussian integration exactly as in the case of a real free field. Of more interest in the present discussion is the two point function. To do this we introduce sources $J(x)$ to define the generating function:

$$Z_p[J] = \int \mathcal{D}\phi \, \exp\left(-S_p[\phi] + \int_{\mathbb{Q}_p} J(x')\phi(x')dx'\right). \tag{4.13}$$

The sources for the 2-point function or propagator take the form of p-adic delta functions at the insertion points x, y are $J(x) = \delta(x' - x) + \delta(x' - y)$. Just as in the real case, we vary with respect to $\phi(x)$ and find the classical solution which extremizes the above action. This is the Green's function for the Vladimirov derivative $G(x - y)$, satisfying

$$\partial_{(p)}G(x - y) = -\delta(x - y). \tag{4.14}$$

To solve for $G(x - y) = \langle 0|\phi(x)\phi(y)|0\rangle$, we apply the p-adic Fourier transform to both sides using techniques from Appendix A. In Fourier space the derivative brings down one power of the momentum

and the delta function becomes an additive character:

$$\widetilde{G}(k) = -\frac{\chi(ky)}{|k|_p}. \tag{4.15}$$

The 2-point function in position space can be obtained by inverse Fourier transform (with $u = x - y$):

$$G(x - y) = -\int_{\mathbb{Q}_p} \frac{\chi(k(y - x))}{|k|_p} dk \tag{4.16}$$

$$= -\int_{\mathbb{Q}_p} \frac{\chi(ku)}{|k|_p} dk. \tag{4.17}$$

This integral is divergent as $k \to 0$. We compute two similar integrals in Appendix B, where the apparent divergence is canceled by the numerator. Unlike in those examples, this integral really does diverge logarithmically, just as the 2-point function of a dimension 0 operator in 2d conformal field theory has a log-divergence. Proceeding as in that case, we introduce a regulator to extract the finite part by computing

$$\lim_{\alpha \to 0} \int_{\mathbb{Q}_p} \chi(ku)|k|_p^{\alpha - 1} dk. \tag{4.18}$$

This appears in the second integral computed in the appendix; in terms of the p-adic gamma function $\Gamma_p(x)$ it is:

$$\lim_{\alpha \to 0} \int_{\mathbb{Q}_p} \chi(ku)|k|_p^{\alpha - 1} dk = \lim_{\alpha \to 0} \Gamma_p(\alpha)|u|_p^{-\alpha}. \tag{4.19}$$

As $\alpha \to 0$ the gamma function has a simple pole and the norm has a log piece:

$$\lim_{\alpha \to 0} \Gamma_p(\alpha) \approx \frac{p - 1}{p \ln p} \frac{1}{\alpha} \tag{4.20}$$

$$\lim_{\alpha \to 0} |u|_p^{-\alpha} \approx 1 - \alpha \ln |u|_p. \tag{4.21}$$

Finally we restore $u = x - y$ and find the 2-point function up to normalization is:

$$\langle 0|\phi(x)\phi(y)|0\rangle \sim \ln\left|\frac{x - y}{a}\right|_p, \quad a \to 0. \tag{4.22}$$

This is exactly analogous to the correlator for the ordinary free boson in two dimensions.

4.2 The Laplacian and harmonic functions on T_p

In addition to boundary scalar fields, we will be interested in scalar fields in the "bulk," i.e., defined on the Bruhat–Tits tree. Such a field is a real- or complex-valued function on the set of vertices. We will

also consider fields that are functions on the set of edges; as we will discuss later, such functions will be analogous to higher-form fields or metric degrees of freedom in the bulk. For now we mention them for completeness and to fix some standard notation. For more information about fields in the tree, the reader can consult [58] and references given therein.

We think of the tree as the 1-skeleton of a simplicial complex, and make use of standard notations and ideas from algebraic topology. The two types of fields mentioned above are just 0- and 1-cochains; we will refer to the space of such objects as $C^*(T_p)$, where $* = 0$ or 1.

If an orientation is chosen on the edges of the tree, the boundary operator acts on its edges by $\partial e = t_e - s_e$, where s and t are the source and target maps. The corresponding coboundary operator acts on fields according to the rule

$$d : C^0(T_p) \to C^1(T_p), \quad (d\phi)(e) = \phi(t_e) - \phi(s_e). \tag{4.23}$$

The formal adjoint of this operator is

$$d^\dagger : C^1(T_p) \to C^0(T_p), \quad (d^\dagger\psi)(v) = \sum_e \pm\psi(e), \tag{4.24}$$

where the sum is over the $p + 1$ edges adjacent to vertex v, with positive sign when v is the source and negative sign when it is the target of e. Whether or not $d^\dagger$ is actually an adjoint to d depends on the class of functions being considered; the L^2 inner product must be well-defined, and boundary conditions at infinity must be chosen to avoid the appearance of a boundary term.

Upon taking the anticommutator $\{d, d^\dagger\}$, we obtain an operator of degree zero, which is the proper analogue of the Laplacian. We will most often use its action on the 0-cochains, which can be represented by the formula

$$\triangle \phi(v) = \sum_{d(v,v')=1} \phi(v') - (p+1)\phi(v). \tag{4.25}$$

This is sometimes written using the notation $\triangle_p = t_p - (p+1)$, where t_p is the Hecke operator on the tree. The analogous formula for 1-cochains is

$$\triangle \psi(e) = \sum_{e'} \pm\psi(e') - 2\psi(e), \tag{4.26}$$

where the sum goes over the $2p$ edges adjacent to e at either side. Unlike for the vertices, there is a dependence on the choice of orientation here: an edge in the sum (4.26) enters with positive sign when it points in the "same direction" as e, i.e., points out from t_e or into s_e. Edges enter with negative sign when the opposite is true. In the standard picture of the tree with ∞ at the top and all finite points of $\mathbb{Q}_p$

at the bottom, oriented vertically, we therefore have exactly one negative term in (4.26), corresponding to the unique edge above e. Notice that, for general p, the Laplacian acting on edges (unlike on vertices) will not have a zero mode; this makes sense, since the tree is a contractible space. The exception is $p = 2$, for which the standard choice of vertical orientations defines a Laplacian which annihilates constant functions of the edges. (Of course, the $p = 2$ tree is still contractible.)

We should remark on one important point: the entire analysis of this paper treats the case where the edges of the tree have uniform lengths, and argues that this is analogous to a maximally symmetric vacuum solution in ordinary gravity. It is natural to wonder what the correct analogues of the metric degrees of freedom actually are. One might speculate that allowing the edge lengths to be dynamical (breaking the $\mathrm{PGL}(2, \mathbb{Q}_p)$ symmetry) should correspond to allowing the metric to vary; after all, this would vary the lengths of paths in the tree, which are the only data that seem logically connected to the metric. By analogy with the Archimedean case, it would then make sense to assume that the edge Laplacian (4.26) will play a role in the linearized bulk equations of motion for edge lengths around a background solution. However, we will relegate further investigation of this idea to future work.

4.2.1 Action functional and equation of motion for scalar fields

Equipped with these ingredients, it is now straightforward to write down action functionals and equations of motion for free scalar fields. The massless quadratic action is

$$S[\phi] = \sum_e |d\phi(e)|^2 \,. \tag{4.27}$$

In what follows, we will study properties of solutions to the "wave equation" $\triangle \phi = 0$, and its massive generalization $(\triangle - m^2)\phi = 0$, on the tree. These have been considered in [58].

There is a family of basic solutions to the Laplace equation, labeled by a choice of a boundary point x and an arbitrary complex number κ. The idea is as follows: Given an arbitrary vertex v in the bulk of the tree, a unique geodesic (indeed, a unique path) connects it to x. As such, exactly one of its $p+1$ neighbors will be closer (by one step) to x, and the other p will be farther by one step. Therefore, the function

$$\varepsilon_{\kappa, x}(v) = p^{-\kappa\, d(x, v)} \tag{4.28}$$

will be an eigenfunction of the Hecke operator, with eigenvalue $(p^\kappa + p^{1-\kappa})$.

The catch in this is that the distance $d(x, v)$ is infinite everywhere in the bulk. We need to regularize it by choosing a centerpoint C in the tree, and declaring that $d(x, C) = 0$. (This just scales the eigenfunction (4.28) by an infinite constant factor). Then $d(x, v) \to -\infty$ as $v \to x$, but we have a well-defined solution to the Laplace equation everywhere in the tree. These solutions are analogous to plane waves;

the solution varies as the exponent of the (regularized) distance to a boundary point, which in the normal archimedean case is just the quantity $\mathbf{k} \cdot \mathbf{r}$.

The corresponding eigenvalue of the Laplacian is

$$\triangle \varepsilon_{\kappa,x} = m_\kappa^2 \varepsilon_{\kappa,x} = \left[(p^\kappa + p^{1-\kappa}) - (p+1) \right] \varepsilon_{\kappa,x}. \tag{4.29}$$

It is therefore immediate that the harmonic functions on the tree (solutions to the massless wave equation) are those with $\kappa = 0$ or 1; $\kappa = 0$ is the zero mode consisting of constant functions, whereas $\kappa = 1$ is the nontrivial zero mode. The eigenvalues (4.29) are invariant under the replacement $\kappa \to 1 - \kappa$, due to the inversion symmetry of the boundary theory.

If we are considering a real scalar field, we must be able to write a basis of real solutions. Of course, when κ is real, we will always be able to do this. More generally, if $\kappa = \kappa_0 + i\gamma$, our solutions look like

$$\varepsilon \sim p^{-\kappa_0 \, d} e^{-i\gamma \ln(p)\, d}, \quad p^{(1-\kappa_0)d} e^{i\gamma \ln(p)\, d}. \tag{4.30}$$

Thus, to construct a basis of real solutions, the following possibilities can occur:

- $\kappa = 1/2$. In this case, there is no restriction on γ, and the solutions look like cosines and sines of $\gamma \ln(p)\, d(x,v)$, modulated by $p^{d(x,v)/2}$.

- $\kappa > 1/2$.[5] In this case, the amplitude parts of the two solutions are linearly independent, and so $\exp(i\gamma \ln(p)\, d)$ must be real. Since d is an integer, the choices are $\gamma \ln(p) = 0$ or π (mod 2π).

While it would be interesting to consider solutions with nonzero γ, we will consider only the one-parameter family of solutions with real κ in the sequel. The parameter m_κ^2 then attains its minimum value for $\kappa = 1/2$. Considering only solutions of this plane-wave form, we therefore have a bound

$$m_\kappa^2 \geq -(\sqrt{p} - 1)^2. \tag{4.31}$$

Note that we could also rewrite (4.29) in the form

$$m_\kappa^2 = -(p+1) + 2\sqrt{p} \cosh \left[\left(\kappa - \frac{1}{2} \right) \ln p \right]. \tag{4.32}$$

4.3 Bulk reconstruction and holography

It is clear from the definition that, when the real part of κ is positive, the plane wave solution (4.28) tends to zero everywhere on the boundary, except at the point x (where it tends to infinity). So we can

---

[5]Due to the $\kappa \mapsto 1 - \kappa$ symmetry, such a choice is always possible.

think of it as representing the solution to the Laplace equation (taking $\kappa = 1$) in the bulk, with specified Dirichlet-type boundary conditions that look like a delta function centered at x. By linearity, we can therefore reconstruct the solution to more general Dirichlet problems by superposition: if the boundary value is to be a certain function $\phi_0(x)$ on $\partial T_p = \mathrm{P}^1(\mathbb{Q}_p)$, then the required bulk harmonic function is

$$\phi(v) = \frac{p}{p+1} \int d\mu_0(x)\, \phi_0(x)\, \varepsilon_{1,x}(v). \tag{4.33}$$

Here $d\mu_0(x)$ is the Patterson-Sullivan measure on $\mathrm{P}^1(\mathbb{Q}_p)$. The normalization factor can be fixed by taking the boundary value to be the characteristic function of any p-adic open ball in the boundary.

We can perform the analogous calculation for massive fields as well, but the sense in which $\phi(v)$ will approach $\phi_0(x)$ as $x \to v$ will be more subtle (since the equation of motion will have no constant mode). Using notation from [58], let $\delta(a \to b, c \to d)$ be the overlap (with sign) of the two indicated oriented paths in the tree, and let

$$\langle v, x \rangle = \delta(C \to v, C \to x) + \delta(v \to x, C \to v). \tag{4.34}$$

This expression makes sense for any bulk vertex v; x may be either a boundary or a bulk point. Note that $\langle z, x \rangle$ is just the negative of the "regularized distance" occurring in our previous discussion.

We would like to compute the bulk solution to the massive equation of motion obtained by integrating our primitive solution (4.28) over its boundary argument, weighted by a boundary function. As a simple choice of boundary function, pick the characteristic function of the p-adic open ball below a vertex w in the tree:

$$\phi_w(v) = \int_{\partial B_w} d\mu_0(x)\, p^{\kappa \langle v, x \rangle}. \tag{4.35}$$

The integral is straightforward to calculate. There are two cases:

$v \notin B_w$ Here, the integrand is constant, and is just equal to $p^{\kappa \langle v, w \rangle}$. The measure of the set over which the integral is performed is $\mu_0(\partial B_w) = p^{-d(C,w)}$, so that the final result is

$$\phi_w(v) = p^{\kappa \langle v, w \rangle - d(C,w)}. \tag{4.36}$$

Note that, if v moves towards the boundary along a branch of the tree, $\langle v, w \rangle$ differs from $-d(C,v)$ by a constant, so that the solution scales as $p^{-\kappa\, d(C,z)}$.

$v \in B_w$ There are now two cases to consider: $x \in B_v$ or $x \notin B_v$. In the first scenario, the integrand is again constant; its value is $p^{\kappa\, d(C,v)}$, and the measure is $\mu_0(B_v) = p^{-d(C,v)}$.

In the second scenario, the geodesic $x \to C$ will meet the geodesic $v \to C$ at a distance h above v; by assumption, $1 \le h \le d(v,w)$. For each value of h, the integrand takes the constant value

39

$p^{\kappa(d(C,v)-2h)}$, and the measure of the corresponding set is

$$\mu(h) = \frac{p-1}{p} p^{-d(C,v)+h}. \tag{4.37}$$

The factor $(p-1)/p$ enters because $p-1$ of the p vertices one step below the meeting vertex correspond to meeting height h (one of them is closer to v). Putting the pieces together, the result is

$$\phi_w(v) = p^{(\kappa-1)d(C,v)} \left(1 + \frac{p-1}{p} \sum_{h=1}^{d(w,v)} \left(p^{1-2\kappa} \right)^h \right)$$

$$= \left(\frac{p^{-2\kappa} - 1}{p^{1-2\kappa} - 1} \right) p^{(\kappa-1)d(C,v)} + \frac{p-1}{p} \left(\frac{p^{(2\kappa-1)d(C,w)}}{p^{2\kappa-1} - 1} \right) p^{-\kappa\, d(C,v)}. \tag{4.38}$$

The reader can check that we recover the correct answer in the massless case, $\kappa \to 1$. Furthermore, our result is a superposition of the asymptotic behavior of the two eigenfunctions corresponding to the mass determined by our original choice of κ. To resolve the ambiguity, we will choose $\kappa > 1/2$.

At this point, we have accumulated enough understanding of scalar fields on the tree to point out how the simplest version of holography will work: namely, classical scalar fields in a non-dynamical AdS background, neglecting backreaction and metric degrees of freedom. In the archimedean case, this version of holography was neatly formulated by Witten [57] in terms of a few simple key facts. Firstly, the coupling between bulk scalar fields and boundary operators must relate the asymptotics (and hence the mass) of the bulk fields to the conformal dimension of the corresponding boundary operators; massless bulk scalars should couple to marginal operators in the boundary CFT. Secondly, the crucial fact that allows the correspondence to work is the existence of a unique solution to the generalized Dirichlet problem for the bulk equations of motion with specified boundary conditions.

Luckily, as we have now shown, all of the important features of the problem persist in the p-adic setting, and Witten's analysis can be carried over kit and caboodle to the tree. In particular, we make his holographic ansatz:

$$\left\langle \int_{\mathrm{P}^1(\mathbb{Q}_p)} d\mu_0 \, \phi_0 \mathscr{O} \right\rangle_{\mathrm{CFT}} = e^{-I_{\mathrm{bulk}}[\phi]}, \tag{4.39}$$

where the bulk field ϕ is the unique classical solution extending the boundary condition ϕ_0, and $\mathscr{O}$ is a boundary operator to which the bulk field couples. In the massless case, where one literally has $\phi_0(x) = \lim_{v\to x} \phi(z)$, $\mathscr{O}$ is an exactly marginal operator in the CFT.

Given our result (4.38), it is simple to write down the correctly normalized bulk-reconstruction formula

for massive fields:

$$\phi(v) = \frac{p^{1-2\kappa} - 1}{p^{-2\kappa} - 1} \int d\mu_0(x) \phi_0(x) p^{\kappa \langle v, x \rangle}, \tag{4.40}$$

$$\phi(v) \sim p^{(\kappa-1)d(C,v)} \phi_0(x) \text{ as } v \to x.$$

When the point v approaches the boundary, the exponent in the kernel becomes

$$\langle v, x \rangle = -d(C, v) + 2\,\mathrm{ord}_p(x - y), \tag{4.41}$$

where y is any boundary point below v. (4.40) then becomes

$$\phi(v) = \left(\frac{p^{1-2\kappa} - 1}{p^{-2\kappa} - 1} \right) p^{-\kappa\, d(C,v)} \int d\mu(x) \frac{\phi_0(x)}{|x - y|_p^{2\kappa}}. \tag{4.42}$$

We can now understand why the Vladimirov derivative is a "normal" derivative on the boundary; it measures the rate of change in the holographic direction of the reconstructed bulk function. In particular, we have that

$$\lim_{v \to y} (\phi(v) - \phi(y)) p^{\kappa d(C,v)} = \left(\frac{p^{1-2\kappa} - 1}{p^{-2\kappa} - 1} \right) \int d\mu(x) \frac{\phi_0(x) - \phi_0(y)}{|x - y|_p^{2\kappa}} = \left(\frac{p^{1-2\kappa} - 1}{p^{-2\kappa} - 1} \right) \partial_{(p)}^{2\kappa-1} \phi(y). \tag{4.43}$$

An argument precisely akin to Zabrodin's demonstration [58] that the bulk action may be written (upon integrating out the interior) as a boundary integral of the nonlocal Vladimirov action shows that we can write $I_{\text{bulk}}[\phi]$ in exactly this form. This demonstrates, exactly as in Witten's archimedean analysis, that a massive field ϕ corresponds to a boundary operator of conformal dimension κ, where $\kappa > 1/2$ is the larger of the two values that correspond to the correct bulk mass. Moreover, the boundary two-point function is proportional to $|x - y|_p^{-2\kappa}$, as expected.

4.4   Scale dependence in bulk reconstruction of boundary modes

Let us consider how the mode expansion of a boundary scalar field interacts with the reconstruction of the corresponding bulk harmonic function. We will be interested in developing the interpretation of the extra, holographic direction as a renormalization scale in our p-adic context. The idea that moving upward in the tree corresponds to destroying information or coarse-graining is already suggested by the identification of the cone above $\mathbb{Z}_p$ (or more generally any branch of the tree) with the inverse limit

$$\mathbb{Z}_p = \varprojlim \mathbb{Z}/p^n \mathbb{Z}, \tag{4.44}$$

where the set of vertices at depth n corresponds to the elements of $\mathbb{Z}/p^n\mathbb{Z}$, and the maps of the inverse system are the obvious quotient maps corresponding to the unique way to move upwards in the tree. A nice intuitive picture to keep in mind is that p-adic integers can be thought of as represented on an odometer with infinitely many $\mathbb{F}_p$-valued digits extending to the left. $\mathbb{Z}/p^n\mathbb{Z}$ is then the quotient ring obtained by forgetting all but n digits, so that there is integer overflow; the maps of the inverse system just forget successively more odometer rings. Since digits farther left are smaller in the p-adic sense, we can think of this as doing arithmetic with finite (but increasing) precision. The parallel to the operation of coarse-graining is apparent; however, we will be able to make it more precise in what follows.

Let's consider a boundary field that is just given by an additive character (plane wave), $\phi_0(x) \sim \exp(2\pi i\{kx\}_p)$. Just as in the complex case, a plane wave in a given coordinate system won't define a solution of fixed wavelength everywhere on $\mathrm{P}^1(\mathbb{C})$; the coordinate transformation (stereographic projection) will mean that the wavelength tends to zero as one moves away from the origin, and the function will become singular at infinity. Therefore, we should instead consider a boundary function of *wavepacket* type, that looks like a plane wave, but supported only in a neighborhood of the origin.

A nice choice to make in the p-adic setting is to take the boundary function to be

$$\phi_0(x) = e^{2\pi i\{kx\}} \cdot \Theta(x, \mathbb{Z}_p), \tag{4.45}$$

where $\Theta(x, S)$ is the characteristic function of the set $S \subset \mathbb{Q}_p$. The transformation (2.17) is actually trivial inside $\mathbb{Z}_p$, so no distortion of the wavepacket occurs at all (unlike for a similar setup in $\mathbb{C}$). Of course, we ought to take $|k|_p > 1$, so that $\{kx\}$ is not constant over the whole of $\mathbb{Z}_p$.

Given this choice of boundary function, the corresponding solution to the bulk equations of motion can be reconstructed using the integral kernel (4.33):

$$\phi(v) = \frac{p}{p+1} \int_{\mathbb{Z}_p} d\mu(x)\, e^{2\pi i\{kx\}} p^{-d_C(x,v)}. \tag{4.46}$$

Recall that $d_C(x, v)$ is the distance from v to x, regularized to be zero at the centerpoint $v = C$ of the tree. We will calculate this integral when v is inside the branch of the tree above $\mathbb{Z}_p$.

Proposition 1. *Let v be a vertex in the branch above $\mathbb{Z}_p$, at a depth ℓ (i.e., since $v \in \mathbb{Z}_p$, distance from the centerpoint) such that $0 \leq \ell < -\operatorname{ord}_p(k) - 2$. Then the reconstructed bulk function $\phi(v)$ is zero.*

Proof. The claim relies on the simple fact that the sum of all p-th roots of unity is zero. Since v is above the red line in Fig. (8) (at depth equal to $-\operatorname{ord}_p(k) - 1$), both terms in the integrand are locally constant below the line, and the integral may be evaluated as a sum along the vertices at the height of the red line. Furthermore, the factor $p^{-d_C(v,x)}$ is constant for each of the p vertices on the line that descend from
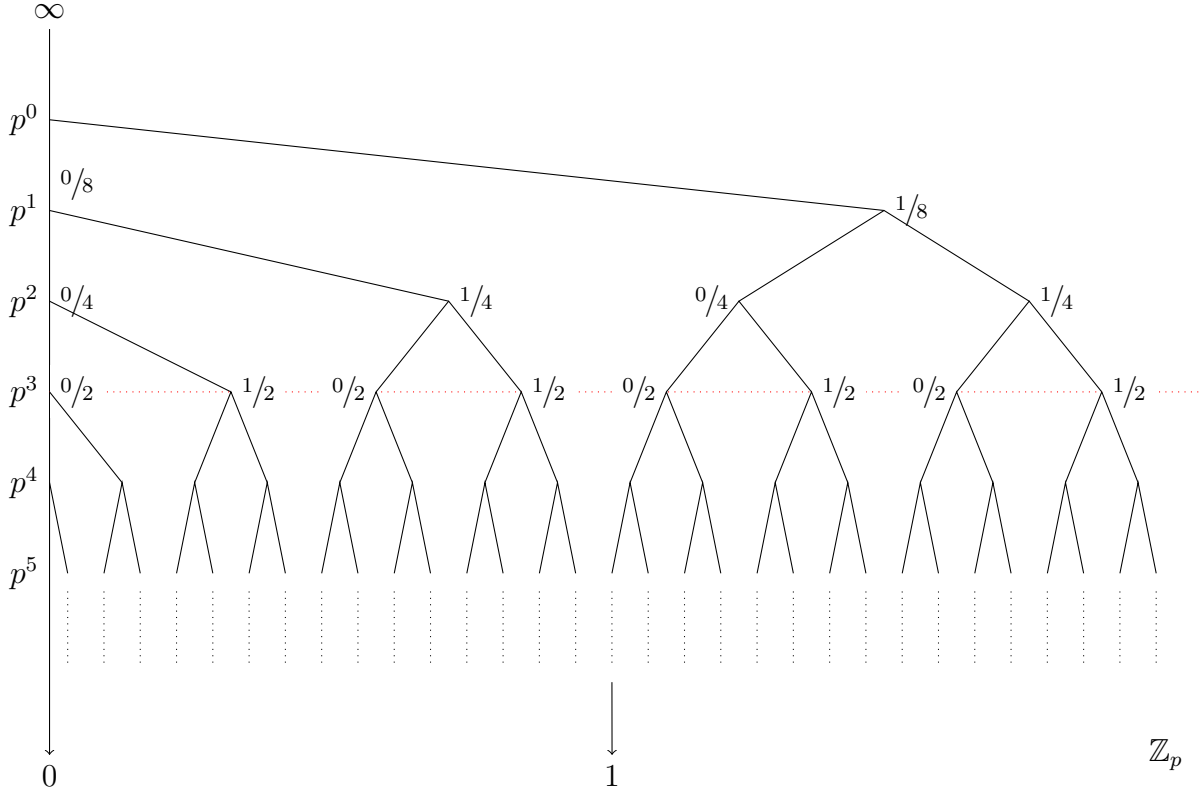
42

Figure 8: A drawing of $\mathbb{Z}_p$ ($p = 2$ for simplicity). Here $k = p^{-4}$. The marked fractions at vertices indicate contributions to $\{kx\}$, which are summed along the geodesic ending at x.

the same ancestor. Since the measure of each branch is equal, the integral is proportional to the sum of all p-th roots of unity, and hence to zero. Notice that this also demonstrates that the reconstructed bulk function is zero everywhere *outside* $\mathbb{Z}_p$: it is zero at the central vertex, and zero on the boundary of the open ball complementary to $\mathbb{Z}_p$. □

Even without calculating the explicit form of the bulk function for vertices below the screening height, this simple argument already allows us to make our physical point: in p-adic holography, the qualitative features of ordinary AdS/CFT persist in a setting where the bulk geometry is discrete, and in some cases are even sharpened. For instance, we have shown explicitly that modes for which $|k|_p$ is large (i.e. the short-wavelength behavior of the boundary conditions) must drop out of the reconstructed bulk field, making exactly zero contribution to it above a height in the tree precisely determined by $|k|_p$. The usual intuition that moving into the bulk along the holographic direction corresponds to integrating out UV modes is thus neatly confirmed.

The explicit form of the reconstructed bulk function at vertices below the screening height is easy to calculate, but less central to our discussion; we leave the computation as an exercise for the reader.

4.5 The possibility of higher-spin fields

We now wish to propose an analogue of higher-spin fields that could be defined in the p-adic case. While we will motivate our proposal here, we do not investigate any properties of p-adic CFT with fields other than scalars. We will return to this question in future work.

We proceed by analogy with two-dimensional CFT, in which the conformal dimension and spin together describe a character of the multiplicative group $\mathbb{C}^\times$:

$$\phi(re^{i\theta} \cdot z) = r^\Delta e^{is\theta} \phi(z). \tag{4.47}$$

The group $\mathbb{C}^\times \simeq \mathbb{R}^\times_{>0} \times \mathrm{U}(1)$; the conformal dimension determines a character of the first factor, and the spin a character of the second, which can be thought of as scale transformations and rotations of the coordinate respectively. The existence of the logarithm function means that we can think of the multiplicative group $\mathbb{R}_+$ as isomorphic to the additive group $\mathbb{R}$.

The structure of the group of units of any local field is understood (see [44] for details). In particular, for the field $\mathbb{Q}_p$, the result is that

$$\mathbb{Q}_p^\times \simeq p^{\mathbb{Z}} \times \mathbb{F}_p^\times \times U^{(1)}, \tag{4.48}$$

where $U^{(1)}$ is the group of "principal units" of the form $1 + p \cdot a$, with $a \in \mathbb{Z}_p$. This decomposition just reflects the structure of the p-adic decimal expansion: since the p-adic norm is multiplicative, any number $x \neq 0$ can be written in the form

$$x = p^{\mathrm{ord}_p(x)} (x_0 + x_1 p + \cdots), \tag{4.49}$$

where $x_0 \neq 0$ (so that $x \in \mathbb{F}_p^\times \simeq C_{p-1}$) and the other x_i may be any digits chosen from $\mathbb{F}_p$. Dividing through by x_0, one gets

$$x = p^{\mathrm{ord}_p(x)} \cdot x_0 \left(1 + \sum_{i \geq 1} \tilde{x}_i p^i\right), \tag{4.50}$$

where $\tilde{x}_i = x_i/x_0$, and the factor in parentheses is a principal unit. A character of $\mathbb{Q}_p^\times$ is therefore a triple of characters, one for each factor in (4.48). The first factor, as in the normal case, corresponds to the scaling dimension of the field; the last two factors are therefore analogous to the spin. Obviously, the second factor corresponds to a $\mathbb{Z}/(p-1)\mathbb{Z}$ phase. It is also known [44] that the set of characters of $U^{(1)}$ is countable and discrete.

In fact, we can naively understand a broader class of the characters of $\mathbb{Z}_p^\times = \mathbb{F}_p^\times \times U^{(1)}$. Recall the description of $\mathbb{Z}_p$ as the inverse limit of its finite truncations:

$$\mathbb{Z}_p = \varprojlim \mathbb{Z}/p^n\mathbb{Z}. \tag{4.51}$$

44

Since this is an inverse limit of rings, there are therefore projection maps between the respective multiplicative groups:

$$\mathbb{Z}_p^\times \to (\mathbb{Z}/p^n\mathbb{Z})^\times \simeq C_{p^{n-1}(p-1)}. \tag{4.52}$$

Therefore, any multiplicative character of a cyclic group $C_{p^{n-1}(p-1)}$ (i.e., any finite root of unity of order $p^{n-1}(p-1)$, for arbitrary n) will give a character of $(\mathbb{Z}/p^n\mathbb{Z})^\times$, which will in turn pull back to define a multiplicative character of the spin part of $\mathbb{Q}_p^\times$. Spin in the p-adic case is therefore both similar to and interestingly different from ordinary two-dimensional CFT.

5 Entanglement entropy

The entanglement entropy in quantum field theories is a notoriously difficult and subtle quantity to compute, and much effort has been expended in developing a toolbox of techniques that provide exact results. One of the first systems in which the computation became tractable was two-dimensional conformal field theory, and in particular the theory of free bosons. Since we are primarily considering the free boson in our discussion, one might hope that the same techniques can be applied in the p-adic case. While we believe that this is the case, and plan to give a full calculation of the entanglement entropy in future work, there are subtleties that arise in each technique and prevent it from being used naively. We will demonstrate these techniques, illustrate the subtle issues that arise, and justify our conjecture for the entanglement entropy in what follows.

As in the real case, we expect the entanglement entropy to have UV divergences. These are normally thought of as localized to the "boundary" of the region under consideration. Care must be used in defining what we mean by interval and boundary; the p-adic numbers have no ordering, and every element of an open set is equally (or equally not) a boundary element.

Whenever possible, we must think in terms of open sets. Over the reals, the open sets are intervals with measure or length given by the norm of the separation distance of the endpoints; as the reader will recall, p-adic open sets are perhaps best visualized using the Bruhat–Tits tree. Once a center C of the tree is picked, we can pick any other vertex v and consider the cone of points below v extending out towards the boundary, which is an open neighborhood in $\mathrm{P}^1(\mathbb{Q}_p)$. A perhaps surprising fact which follows from the definition of the p-adic norm $|x - y|_p$ ($x, y \in \mathrm{P}^1(\mathbb{Q}_p)$) is that it is related to the height of the cone required to connect x to y (see Fig. 9).

Following standard arguments, say of [51, 16], we can pick the boundary cone below the point v to be called the region V. The total Hilbert space on $\mathbb{Q}_p$ splits into Hilbert spaces on V and its complement, $\mathcal{H} = \mathcal{H}_V \otimes \mathcal{H}_{-V}$. The entanglement entropy defined by $S(V) = -\operatorname{tr}(\rho_V \log \rho_V)$ and by construction satisfies $S(V) = S(-V)$. As there are an infinite number of points $x_i \in V \in \mathrm{P}^{1^1}(\mathbb{Q}_p)$, there is an unbounded number

45

of local degrees of freedom $\phi(x_i)$ as is typical of quantum field theory. In the continuum case this implies logarithmic divergences from modes in V entangled with those in $-V$, and we expect the same to be true in the p-adic case.

In the works of Cardy and Calabrese [12, 13], the entanglement entropy for intervals in $1+1$-dimensional conformal field theories are explicitly calculated. The p-adic field theories considered here are exactly analogous to the two-dimensional free boson; in both, the scalar $\phi(x)$ has conformal dimension zero and (as we have shown above) a logarithmically divergent propagator. We wish to understand how much of their calculation can be duplicated in the p-adic case. These authors generally follow a series of steps beginning with the replica trick, which is the observation that n powers of the reduced density matrix ρ_V can be computed by evaluating the partition function on a Riemann surface obtained by gluing n copies of the theory together along the interval V. The entanglement entropy follows from analytic continuation of these results in n, followed by the limit $n \to 1$, according to the formula

$$\text{tr}(\rho_V^n) = \frac{Z_n(V)}{Z_1^n}, \quad S_V = -\lim_{n \to 1} \frac{\partial}{\partial n} \frac{Z_n(V)}{Z_1^n}, \tag{5.1}$$

where $Z_n(V)$ is the n-sheeted partition function and Z_1 is the partition function of 1 sheet with no gluing, which is required for normalization.

In $1+1$ dimensions, the n sheeted partition function can be viewed as a Riemann surface, and the holomorphic properties of this surface make the calculation tractable. In particular, if the interval has the boundary points x and y, the complicated world sheet topology can be mapped to the target space by defining multi-valued *twist fields* $\Phi_n(x), \Phi_n(y)$ on the plane whose boundary conditions implement the n sheeted surface. One can find that $\text{tr}(\rho_V^n)$ behaves exactly like the nth power of a two point function of the twist fields, once their conformal dimension has been determined using Ward identities:

$$\text{tr}(\rho_V^n) \sim \langle 0 | \Phi_n(x) \Phi_n(y) | 0 \rangle^n \sim \left(\frac{x-y}{\epsilon} \right)^{-\frac{c}{6}\left(n - \frac{1}{n}\right)} \tag{5.2}$$

where c is the central charge and ϵ is a normalization constant from Z_1. When $n = 1$ exactly, the twist fields have scaling dimension 0 and the above correlator no longer makes sense. Instead, taking the limit as $n \to 1$, the linear term is $-n\frac{c}{3} \ln \left(\frac{x-y}{\epsilon} \right)$. Taking the derivative gives the famous universal formula for the entanglement entropy [30].

The difficulty in performing the same calculation over the p-adics consists in fixing the dimensions of the twist operators. These operators can be defined just as in the normal case; after all, all that they do is implement certain boundary conditions at branch points on the fields in a theory of n free bosons. However, the usual arguments that fix their dimension rely on the existence of a uniformizing transformation $z \mapsto z^n$

that describes the relevant n-sheeted branched cover of P^1 by P^1; the Schwarzian of this holomorphic (but not Möbius) transformation then appears as the conformal dimension. The argument using the OPE with the stress tensor is identical in content. Both cases rely on the existence of holomorphic (but not fractional-linear) transformations, and a measure—the Schwarzian or conformal anomaly—of their "failure" to be Möbius.

In the p-adic case, this is related to the question of local conformal transformations; it has been suggested [42] that no such symmetries exist. Moreover, since $\mathbb{Q}_p$ is not algebraically closed, a transformation like $z \mapsto z^n$ need not even be onto. Nevertheless, we can still define the twist operators, and we suppose that they transform as primaries with some conformal dimensions Δ_n. Their two-point function then gives the density matrix. This function is:

$$\langle 0|\Phi_n^{(p)}(x)\Phi_n^{(p)}(y)|0\rangle^n \sim \left|\frac{x-y}{\epsilon}\right|_p^{-2n\Delta_n} \tag{5.3}$$

where Δ_n are the model-dependent (and unknown) conformal dimensions. Inserting this ansatz into $-\lim_{n\to 1}\frac{\partial}{\partial n}\operatorname{tr}(\rho_V^n)$ and taking the limit $n \to 1$, $\Delta_n \to 0$ gives:

$$\left(2n\frac{\partial \Delta_n}{\partial n}\Big|_{n=0}\right)\ln\left|\frac{x-y}{\epsilon}\right|_p. \tag{5.4}$$

While this is not a proof, it provides some evidence for the expected logarithmic scaling of the entropy. We expect that the dimensions $\Delta_n \to 0$ as $n \to 1$, since of course the twist operator on one sheet is just the identity. If we could fix the conformal dimension without using the conformal anomaly, this calculation would fix not only the logarithmic form of the answer, but also the coefficient that plays the role of the central charge. It may be possible to do this by examining the path integral with twist-operator insertions directly.

A possible way around this difficulty might be to consider a harder problem first: to think about two intervals rather than one. The genus of the Riemann surface that appears in the replica trick is $g = (n-1)(N-1)$; thus, for one interval, we are considering a branched cover of P^1 over itself, and the conformal anomaly is a necessary ingredient. However, one might hope that for two intervals, we can simply compute the partition function on a series of higher-genus Riemann surfaces (which is understood in the p-adic case), and take the limit as the genus approaches zero. Discussions of the entanglement entropy in terms of Schottky uniformization—which therefore appear tailored to our needs—have appeared in the literature [22].

Two difficulties appear in this case: the first is matching the moduli of the Riemann surface in question to the lengths of the intervals; the second is more subtle, and reflects the fact that, over the p-adics, not

every branched cover of P^1 is a Mumford curve [9]. We believe that one of the strategies outlined here will succeed in producing a rigorous computation of the entanglement entropy, but we must relegate that computation to future work.

5.1 Ryu-Takayanagi formula

Let us take as given the conjecture from the previous section that the entanglement entropy of a region in the boundary CFT should be computed as the logarithm of its p-adic size. We take our interval to be the smallest p-adic open ball which contains points x and y. This interval has size $|x - y|_p$. To understand the Ryu-Takayanagi formula, it remains to compute the length of the unique geodesic connecting x to y. The tree geometry for this setup is depicted in Fig. 9. Since there are an infinite number of steps required to reach the boundary, the geodesic length is formally infinite, just as in the real case. We regulate this by cutting off the tree at some finite tree distance a from the center C, which can be thought of as $\mathrm{ord}_p(\epsilon)$ for some small p-adic number ϵ. We will then take this minimum number $\epsilon \to 0$ (p-adically). This limit will push the cutoff in the tree to infinite distance from C.

A $SL(2, \mathbb{Q}_p)$ transformation can always be used to move the points x and y to the $\mathbb{Z}_p$ part of the tree first to simplify the argument. Then introducing the distance cutoff a effectively truncates the decimal expansions of x and y to the first a decimal places. In the case where $|x - y|_p = 1$, the geodesic connecting the two points passes through C and has length $2a$. If $|x - y|_p < 1$, the geodesic is shorter by a factor of $2d$, where $|x - y|_p = p^{-d}$. Roughly speaking, as can be seen in Fig. 9, smaller boundary regions are subtended by shorter geodesics in the tree.

We see that the cutoff-dependent distance is

$$d(x, y)_a = 2a + \frac{2}{\ln p} \ln |x - y|_p. \tag{5.5}$$

We would like to take $a \to \infty$. Up to the factor of $\ln p$, we can define a to be the logarithm of a p-adic cutoff ϵ such that $a \to \infty$ as $\epsilon \to 0$. Using this definition, we find the length of a boundary-anchored geodesic to be

$$d(x, y) = \lim_{\epsilon \to 0} \frac{2}{\ln p} \ln \left| \frac{x - y}{\epsilon} \right|_p. \tag{5.6}$$

Up to the overall factor in front (which presumably depended on our choice of the length of each leg of the tree), we see the geodesic length is logarithmically divergent in interval size.
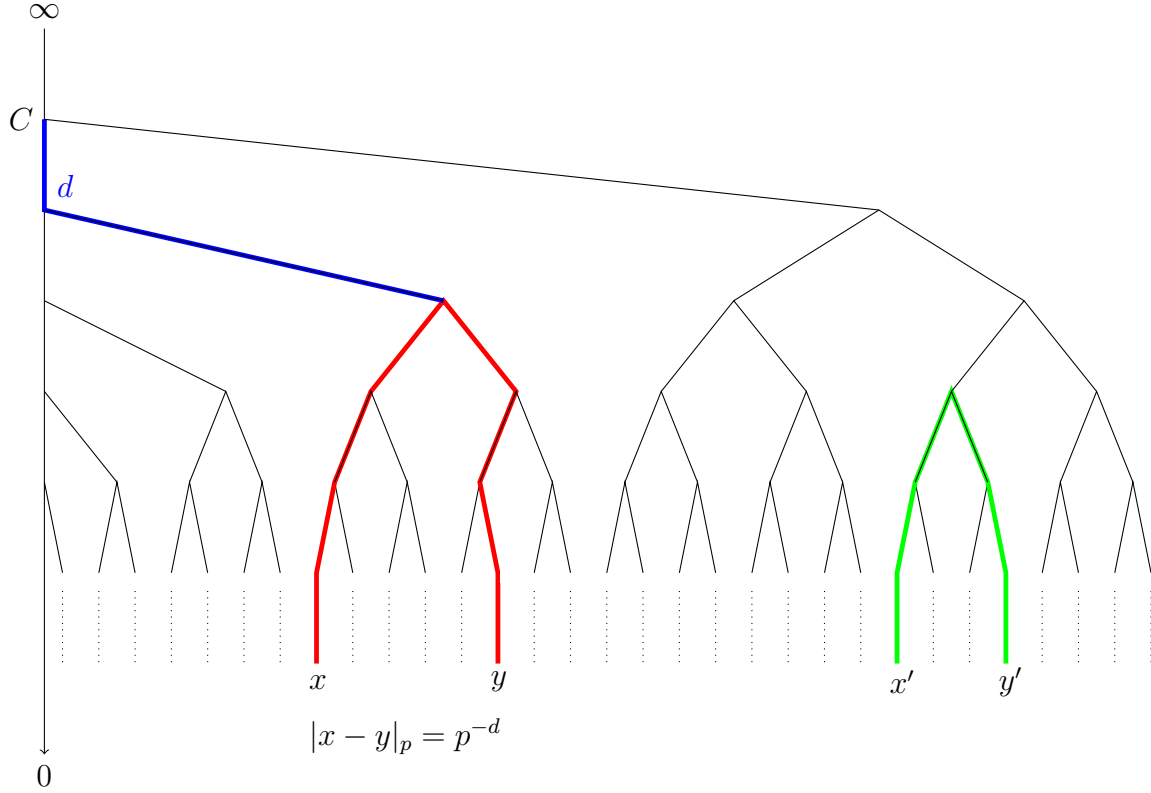
Figure 9: Boundary anchored geodesics in T_p have a natural interpretation in terms of the p-adic norm. Once the arbitrary position of the center C is fixed, the norm of open sets in $\mathbb{Q}_p$ is given by p^{-d}, where d is the integer number of steps from C required before the path to the endpoints splits. In this example, $|x-y|_p$ is described by the red geodesic and the value is p^{-2}. The set corresponding to the green geodesic has a smaller norm by a factor of p because the vertex is 1 step further down the tree. As in the case of real AdS, the length of the geodesic is formally infinite because an infinite number of steps is required to reach the boundary. One may introduce a cutoff corresponding to truncation of the tree at a fixed distance, then take the limit as this cutoff goes to zero. It should be apparent that the (formally infinite) red geodesic is longer than the green one by two steps. Up to constant factors, the length of any boundary-anchored geodesic is an infinite term minus d. This explains the logarithmically divergent scaling of geodesic length with p-adic norm.

5.2 An adelic formula for entanglement?

We have argued that the general form of entanglement entropy scaling for the boundary theory is dual to a geodesic length in the bulk. At the present time we lack a p-adic notion of central charge c or theory dependent quantity which counts boundary degrees of freedom. Nevertheless, we claim the general form is

$$S_p(x - y) = c_p \ln \left| \frac{x - y}{\epsilon_p} \right|_p . \tag{5.7}$$

We now wish to speculate about the possibility of an *adelic* formula for the entanglement entropies.

In the study of p-adic numbers, there exists a surprising formula which relates the various p-adic valuations of a rational number to its real norm. This is a different form of the fundamental theorem of arithmetic, and is sometimes known as an adelic formula:

$$\prod_p^\infty |x|_p = 1. \tag{5.8}$$

Here $x \in \mathbb{Q}$ and the product is taken over all primes. The "prime at ∞" corresponds to the usual archimedean norm $|x|_\infty = |x|$. This equality follows by considering the unique prime factorization of x into a product of prime powers. When x contains a factor p^n, then $|x|_p = p^{-n}$. This means the infinite product over primes is well defined because only finitely many terms are not equal to 1. In fact, the product over the finite primes gives exactly the inverse of the real norm $|x|$. Therefore the product over all finite places and the infinite place is unity.

We now wish to again recall the familiar formula for the universal entanglement entropy of an interval in a 1+1 dimensional conformal field theory; written suggestively in the "prime at infinity" notation:

$$S_\infty(x - y) = \frac{c}{3} \ln \left| \frac{x - y}{\epsilon_\infty} \right|_\infty . \tag{5.9}$$

One might hope through a better understanding of p-adic conformal field theory or the holographic dual, the value of the proportionality constant or the p-adic central charge might be determined. In the (perhaps unlikely) event that the central charges of the p-adic theory agree with the real case, then using the adelic formula for the interval, we propose:

If $c_p = c/3$ for all p and $x - y \in \mathbb{Q}$, then

$$\sum_p^\infty S_p(x - y) \propto \ln \left(\prod_p^\infty \left| \frac{x - y}{\epsilon_p} \right|_p \right) = 0. \tag{5.10}$$

50

One might be suspicious about this formula; each of the entropies S_p are formally divergent. Additionally, since these quantities are entropies they are expected to be positive. Therefore care must be taken in interpreting the above.

One possible resolution is the erroneous application of the adelic formula to the cutoffs ϵ_p. In computing S_p holographically, we assumed $|\epsilon|_p \to 0$. However, if $|\epsilon_p|_p \to 0$ in one norm, it is not generally true that $|\epsilon_p|_{p'} \to 0$ for another choice p'. Therefore, we require a numerically different cutoff parameter ϵ_p for each system over p. As all these parameters are taken to 0 in their respective norms, the corresponding entanglement entropies diverge.

Understanding that the cut offs ϵ_p do not cancel on the left or right hand sides, we are left with the divergent pieces of the entropy being equal on both sides. However, if we vary the length of $|x - y|_\infty$ in the real physical system, we see that the entropy difference associated with this interval is distributed across the S_p's such that the sum is zero. Put another way, varying the real interval length will cause some values of $|x - y|_p$ for different p to increase and others to decrease. This causes some S_p to increase and others to decrease such that the total change of entropy over all finite and infinite places is 0.

We will leave it to future work to try to derive or understand this relation further.

6 p-adic bulk geometry: Schottky uniformization and non-archimedean black holes

6.1 Holography for Euclidean higher-genus black holes

The first explicit form of AdS/CFT correspondence for the asymptotically AdS$_3$ higher genus black holes, in the Euclidean signature, was obtained in [40], where the computation of the Arakelov Green function of [36] is shown to be a form of the holographic correspondence for these black holes, where the two-point correlation function for a field theory on the conformal boundary X_Γ is written in terms of gravity in the bulk $\mathcal{H}_\Gamma$, as a combination of lengths of geodesics.

At the heart of Manin's holographic formula lies a simple identity relating conformal geometry on $\mathrm{P}^1(\mathbb{C})$ and hyperbolic geometry on $\mathbf{H}^3$, namely the fact that the cross ratio of four points on the boundary $\mathrm{P}^1(\mathbb{C})$ can be written as the length of an arc of geodesic in the bulk $\mathbf{H}^3$. More precisely, consider the two point correlation function $g(A, B)$ on $\mathrm{P}^1(\mathbb{C})$. This is defined by considering, for a divisor $A = \sum_x m_x x$, the Green function of the Laplacian

$$\partial \bar{\partial} g_A = \pi i (\deg(A) d\mu - \delta_A),$$

with δ_A the delta current associated to the divisor, $\delta_A(\varphi) = \sum_x m_x \varphi(x)$, and $d\mu$ a positive real-analytic 2-form. The Green function g_A has the property that $g_A - m_x \log |z|$ is real analytic for z a local coordinate

near x, and is normalized by $\int g_A d\mu = 0$. For two divisors A, B, with A as above and $B = \sum_y n_y\, y$ the two point function is given by $g(A, B) = \sum_y n_y g_A(y)$. For degree zero divisors it is independent of the form $d\mu$ and is a conformal invariant. If w_A is a meromorphic function on $\mathrm{P}^1(\mathbb{C})$ with $Div(w_A) = A$, and C_B is a 1-chain with boundary B, the two point function satisfies

$$g(A, B) = Re \int_{C_B} \frac{dw_A}{w_A}.$$

For (a, b, c, d) a quadruple of points in $\mathrm{P}^1(\mathbb{C})$, the cross ratio $\langle a, b, c, d \rangle$ satisfies

$$\langle a, b, c, d \rangle = \frac{w_{(a)-(b)}(c)}{w_{(a)-(b)}(d)},$$

where $(a) - (b)$ is the degree zero divisor on $\mathrm{P}^1(\mathbb{C})$ determined by the points a, b, and the two point function is

$$g((a) - (b), (c) - (d)) = \log \frac{|w_{(a)-(b)}(c)|}{|w_{(a)-(b)}(d)|}.$$

Given two points a, b in $\mathrm{P}^1(\mathbb{C})$, let $\ell_{\{a,b\}}$ denote the unique geodesics in $\mathbf{H}^3$ with endpoints a and b. Also given a geodesic ℓ in $\mathbf{H}^3$ and a point $c \in \mathrm{P}^1(\mathbb{C})$ we write $c * \ell$ for the point of intersection between ℓ and the unique geodesic with an endpoint at c and intersecting ℓ orthogonally. We also write $\lambda(x, y)$ for the oriented distance of the geodesic arc in $\mathbf{H}^3$ connecting two given points x, y on an oriented geodesic. Then the basic holographic formula identifies the two point function with the geodesic length

$$g((a) - (b), (c) - (d)) = -\lambda(a * \ell_{\{c,d\}}, b * \ell_{\{c,d\}}).$$

One can also express the argument of the cross ratio in terms of angles between bulk geodesics (see [36], [40]). This basic formula relating the two point correlation function on the boundary to the geodesic lengths in the bulk is adapted to the higher genus cases by a suitable procedure of averaging over the action of the group that provides an explicit construction of a basis of meromorphic differentials on the Riemann surface X_Γ in terms of cross ratios on $\mathrm{P}^1(\mathbb{C})$. A basis of holomorphic differentials on X_Γ, with

$$\int_{A_k} \omega_{\gamma_j} = 2\pi i \delta_{jk}, \qquad \int_{B_k} \omega_{\gamma_j} = \tau_{jk}$$

the period matrix, is given by

$$\omega_{\gamma_i} = \sum_{h \in S(\gamma_i)} d_z \log \langle z_h^+, z_h^-, z, z_0 \rangle,$$

for $z, z_0 \in \Omega_\Gamma$, with $S(\gamma)$ the conjugacy class of γ in Γ. The series converges absolutely when $\dim_H(\Lambda_\Gamma) < 1$.

Meromorphic differentials associated to a divisor $A = (a) - (b)$ are similarly obtained as averages over the group action

$$\nu_{(a)-(b)} = \sum_{\gamma \in \Gamma} d_z \log \langle a, b, \gamma z, \gamma z_0 \rangle$$

and the Green function is computed as a combination $\nu_{(a)-(b)} - \sum_j X_j(a,b) \omega_{\gamma_j}$ with the coefficients $X_j(a,b)$ so that the B_k-periods vanish. Since in the resulting formula each crossed ratio term is expressible in terms of the length of an arc of geodesic in the bulk, the entire Green function is expressible in terms of gravity in the bulk space. We refer the reader to §§2.3, 2.4, and 2.5 of [40] and to [41] for a more detailed discussion and the resulting explicit formula of the holographic correspondence for arbitrary genus.

6.2 Holography on p-adic higher genus black holes

In the special case of a genus-one curve, the relevant Schottky group is isomorphic to $q^{\mathbb{Z}}$, for some $q \in \mathbf{k}^*$, and the limit set consists of two points, which we can identify with 0 and ∞ in $\mathrm{P}^1(\mathbf{k})$. The generator of the group acts on the geodesic in $T_{\mathbf{k}}$ with endpoints 0 and ∞ as a translation by some length $n = \log|q| = v_{\mathfrak{m}}(q)$, the valuation. The finite graph $G_{\mathbf{k}}$ is then a polygon with n edges, and the graph $T_{\mathbf{k}}/\Gamma$ consists of this polygon with infinite trees attached to the vertices. The boundary at infinity of $T_{\mathbf{k}}/\Gamma$ is a Mumford curve $X_\Gamma(\mathbf{k})$ of genus one with its p-adic Tate uniformization. The graph $T_{\mathbf{k}}/\Gamma$ is the p-adic BTZ black hole, with the central polygon $G_{\mathbf{k}}$ as the event horizon. The area of the black hole and its entropy are computed by the length of the polygon (see Fig. 10).

The higher genus cases are p-adic versions of the higher genus black holes discussed above, with the finite graph $G_{\mathbf{k}}$ as event horizon, and its geodesic length proportional to the black hole entropy.

Given a set of generators $\{\gamma_1, \ldots, \gamma_g\}$ of a p-adic Schottky group, let n_{γ_i} be the translation lengths that describe the action of each generator γ_i on its axis ℓ_{γ_i}. More precisely, if an element γ is conjugate in $\mathrm{PGL}(2, \mathbf{k})$ to an element of the form

$$\begin{pmatrix} q & 0 \\ 0 & 1 \end{pmatrix},$$

then the translation length is $n_\gamma = v_{\mathfrak{m}}(q) = \mathrm{ord}_{\mathbf{k}}(q)$, the order (valuation) of q. The translation lengths $\{n_{\gamma_i}\}$ are the Schottky invariants of the p-adic Schottky group Γ. It is shown in [15] that the Schottky invariants can be computed as a spectral flow.

The Drinfeld–Manin holographic formula of [35] for p-adic black holes of arbitrary genus is completely analogous to its archimedean counterpart of [36]. There is a good notion of $\mathbf{k}$-divisor on $\mathrm{P}^1(\mathbf{k})$, as a function $\mathrm{P}^1(\bar{\mathbf{k}}) \to \mathbb{Z}$, with $z \mapsto m_z$, with the properties that $m_{z_1} = m_{z_2}$ if z_1 and z_2 are conjugate over $\mathbf{k}$; that all points z with $m_z \neq 0$ lie in the set of points of P^1 over a finite extension of $\mathbf{k}$; and that the set of points with $m_z \neq 0$ has no accumulation point. As before we write such a divisor as $A = \sum_z m_z z$. Given
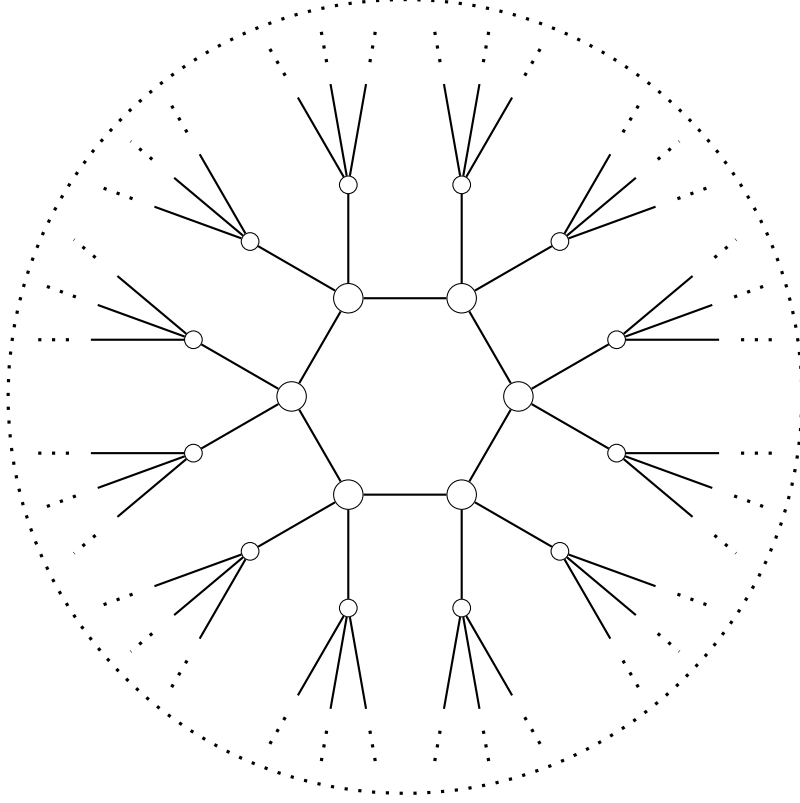
Figure 10: The p-adic BTZ black hole. (As pictured, $p = 3$).

a Γ-invariant divisor A of degree zero, there exists a meromorphic function on $\Omega_\Gamma(\mathbf{k})$ with divisor A. It is given by a Weierstrass product

$$W_{A,z_0} = \prod_{\gamma \in \Gamma} \frac{w_A(\gamma z)}{w_A(\gamma z_0)},$$

where $w_A(z)$ is a $\mathbf{k}$-rational function on $\mathrm{P}^1(\mathbf{k})$ with divisor A. The convergence of this product is discussed in Proposition 1 of [35]: the non-archimedean nature of the field $\mathbf{k}$ implies that the product converges for all $z \in \Omega_\Gamma \setminus \cup_\gamma \gamma(\mathrm{supp}(A))$. The function W_{A,z_0} is a p-adic automorphic function (see [39]) with $W_{A,z_0}(\gamma z) = \mu_A(\gamma) W_{A,z_0}(z)$, with $\mu_A(\gamma) \in \mathbf{k}^*$, multiplicative in A and γ. One obtains a basis of Γ-invariant holomorphic differentials on $X_\Gamma(\mathbf{k})$ by taking

$$\omega_{\gamma_i} = d \log W_{(\gamma_i - 1)z_0, z_1},$$

where

$$W_{(\gamma-1)z_0, z_1}(z) = \prod_{h \in C(\gamma)} \frac{w_{hz_\gamma^+ - hz_\gamma^-}(z)}{w_{hz_\gamma^+ - hz_\gamma^-}(z_0)},$$

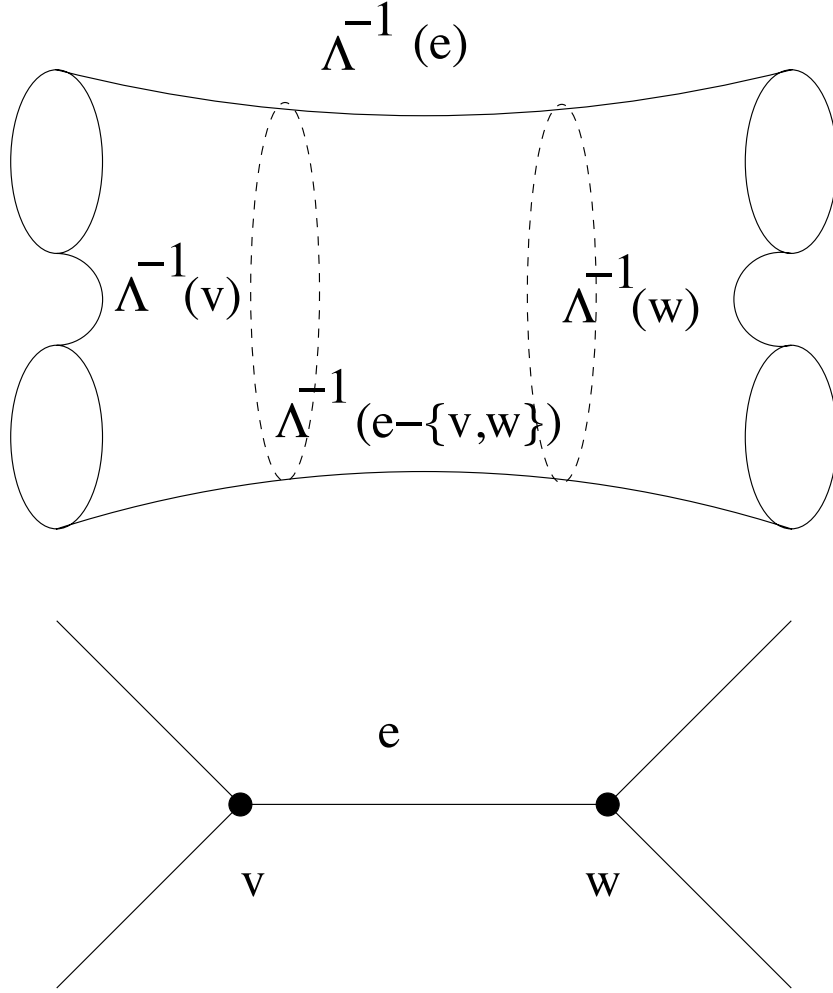for $C(g)$ a set of representatives of $\Gamma/\gamma^{\mathbb{Z}}$.

54

Figure 11: Drinfeld's p-adic upper half plane and the Bruhat–Tits tree.

It is shown in [35] that the order of the cross ratio on $\mathrm{P}^1(\mathbf{k})$ is given by

$$\mathrm{ord}_{\mathbf{k}} \frac{w_A(z_1)}{w_A(z_2)} = \#\{\ell_{z_1,z_2}, \ell_{a_1,a_2}\},$$

for $A = a_1 - a_2$ and $\ell_{x,y}$ the geodesic in the Bruhat–Tits tree with endpoints $x, y \in \mathrm{P}^1(\mathbf{k})$, with $\#\{\ell_{z_1,z_2}, \ell_{a_1,a_2}\}$ the number of edges in common to the two geodesics in $T_{\mathbf{k}}$. This is the basic p-adic holographic formula relating boundary two point function to gravity in the bulk.

A difference with respect to the Archimedean case is that, over $\mathbb{C}$, both the absolute value and the argument of the cross ratio have an interpretation in terms of geodesics, with the absolute value expressed in terms of lengths of geodesic arcs and the argument in terms of angles between geodesics, as recalled above. In the p-adic case, however, it is only the valuation of the two point correlation function that has

an interpretation in terms of geodesic lengths in the Bruhat–Tits tree. The reason behind this discrepancy between the archimedean and non-archimedean cases lies in the fact that the Bruhat–Tits tree $T_\mathbf{k}$ is the correct analog of the hyperbolic handlebody $\mathbf{H}^3$ only for what concerns the part of the holographic correspondence that involves the absolute value (respectively, the p-adic valuation) of the boundary two point function. There is a more refined p-adic space, which maps surjectively to the Bruhat–Tits tree, which captures the complete structure of the p-adic automorphic forms for the action of a p-adic Schottky group Γ: Drinfeld's p-adic upper half plane, see Chapter I of [7]. Given $\mathbf{k}$ as above, let $\mathbb{C}_p$ denote the completion of the algebraic closure of $\mathbf{k}$. Drinfeld's p-adic upper half plane is defined as $\mathbf{H_k} = \mathrm{P}^1(\mathbb{C}_p) \setminus \mathrm{P}^1(\mathbf{k})$. One can view this as an analog of the upper and lower half planes in the complex case, with $\mathbf{H}^+ \cup \mathbf{H}^- = \mathrm{P}^1(\mathbb{C}) \setminus \mathrm{P}^1(\mathbb{R})$. There is a surjection $\lambda : \mathbf{H_k} \to T_\mathbf{k}$, defined in terms of the valuation, from Drinfeld's p-adic upper half plane $\mathbf{H_k}$ to the Bruhat–Tits tree $T_\mathbf{k}$. For vertices $v, w \in V(T_\mathbf{k})$ connected by an edge $e \in E(T_\mathbf{k})$, the preimages $\lambda^{-1}(v)$ and $\lambda^{-1}(w)$ are open subsets of $\lambda^{-1}(e)$, as illustrated in Fig. 11. The map $\lambda : \mathbf{H_k} \to T_\mathbf{k}$ is equivariant with respect to the natural actions of $\mathrm{PGL}(2, \mathbf{k})$ on $\mathbf{H_k}$ and on $T_\mathbf{k}$. In particular, given a p-adic Schottky group $\Gamma \subset \mathrm{PGL}(2, \mathbf{k})$, we can consider the quotients $\tilde{\mathcal{H}}_\Gamma = \mathbf{H_k}/\Gamma$ and $\mathcal{H}_\Gamma = T_\mathbf{k}/\Gamma$ and the induced projection $\lambda : \tilde{\mathcal{H}}_\Gamma \to \mathcal{H}_\Gamma$. Both quotients have conformal boundary at infinity given by the Mumford curve $X_\Gamma = \Omega_\Gamma(\mathbf{k})/\Gamma$, with $\Omega_\Gamma(\mathbf{k}) = \mathrm{P}^1(\mathbf{k}) \setminus \Lambda_\Gamma$, the domain of discontinuity of the action of Γ on $\mathrm{P}^1(\mathbf{k}) = \partial \mathbf{H_k} = \partial T_\mathbf{k}$. One can view the relation between $\mathbf{H_k}$ and $T_\mathbf{k}$ illustrated in Fig. 11, and the corresponding relation between $\tilde{\mathcal{H}}_\Gamma$ and $\mathcal{H}_\Gamma$, by thinking of $\tilde{\mathcal{H}}_\Gamma$ as a "thickening" of the graph $\mathcal{H}_\Gamma$, just as in the Euclidean case one can view the union of the fundamental domains of the action of Γ on $\mathbf{H}^3$, as illustrated in Fig. 4, as a thickening of the Cayley graph (tree) of the Schottky group Γ, embedded in $\mathbf{H}^3$.

Thus, when considering the non-archimedean holographic correspondence and p-adic black holes of arbitrary genus, one can choose to work with either $\mathcal{H}_\Gamma$ or with $\tilde{\mathcal{H}}_\Gamma$ as the bulk space, the first based on Bruhat–Tits trees and the second (more refined) based on Drinfeld's p-adic upper half spaces. In this paper we will be focusing on those aspects of the non-archimedean AdS/CFT correspondence that are captured by the Bruhat–Tits tree, while we will consider a more refined form of non-archimedean holography, based on Drinfeld's p-adic upper half planes, in forthcoming work.

6.3 Scalars on higher-genus backgrounds: sample calculation

In light of this discussion of higher-genus holography in the p-adic case, it is easy to understand how to generalize the arguments and calculations we discussed for scalar fields in §4 to the BTZ black hole, or to higher-genus hyperbolic handlebodies, the p-adic analogues of Krasnov's Euclidean black holes. One can simply think of the higher-genus geometry as arising from the quotient of the tree T_p (and its boundary $\mathrm{P}^1(\mathbb{Q}_p)$) by the action of a rank-g Schottky group. Any quantity that can then be made equivariant under the action of the Schottky group will then descend naturally to the higher-genus setting.
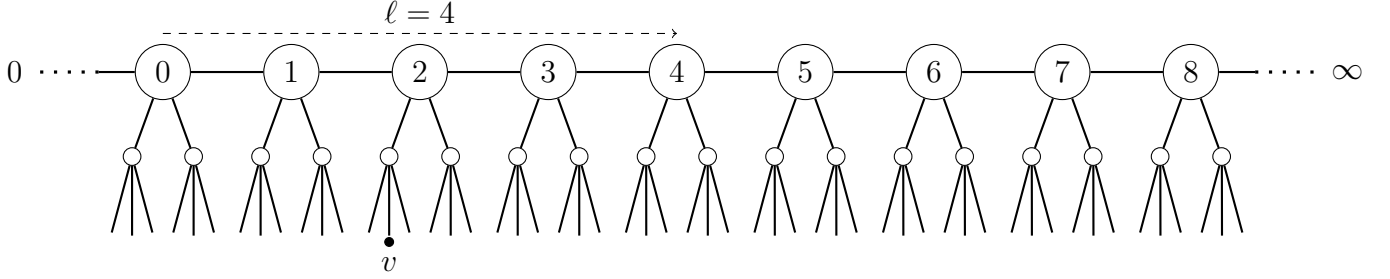
Figure 12: The action of a rank-one Schottky group (translation by ℓ along a fixed geodesic) on the Bruhat–Tits tree. As pictured, $n = h = 2$.

As a simple example, it is easy to construct the genus-1 analogue of our basic Green's function (4.28), using the method of images. We perform this calculation in the following paragraphs. The result makes it easy to perform the reconstruction of bulk solutions to the equations of motion in a BTZ background, with specified boundary conditions at infinity along the genus-1 conformal boundary.

Without loss of generality, we can label the distance along the geodesic which is translated by the chosen Schottky generator by integers, and imagine that the source is attached at a boundary point x connected to the vertex 0. The bulk vertex v at which we want to evaluate the Green's function will be attached to vertex n ($0 \leq n < \ell$), at a depth h from the central geodesic. The quantity to be calculated is simply

$$\varepsilon_{\kappa,x}^{(g=1)}(v) = \sum_{g \in \mathbb{Z}} p^{\kappa \langle v, gx \rangle}, \tag{6.1}$$

where the sum ranges over the images of x under the Schottky group. We take the integrand to be normalized to 1 at the vertex where the branch containing x meets the central geodesic. The cases $n = 0$ and $n \neq 0$ are different, and we will treat them separately.

$n = 0$: In this case, the sum becomes

$$\varepsilon_{\kappa,x}(v) = p^{\kappa \langle v, x \rangle} + 2 \sum_{m>0} \left(p^{-\kappa \ell} \right)^m$$

$$= p^{\kappa \langle v, x \rangle} + \frac{2 p^{-\kappa h}}{p^{\kappa \ell} - 1}. \tag{6.2}$$

$n \neq 0$: In this case, the sum becomes

$$\varepsilon_{\kappa,x}(v) = \sum_{m \leq 0} p^{\kappa(-n-h-|m|\ell)} + \sum_{m>0} p^{\kappa(n-h-m\ell)}$$

$$= p^{-\kappa h} \left(\frac{p^{\kappa(\ell-n)} + p^{\kappa n}}{p^{\kappa \ell} - 1} \right). \tag{6.3}$$

57

In both cases, the result has the expected boundary behavior: it falls off asymptotically as $p^{-\kappa h}$ when v approaches any boundary point other than x itself.

7   Conclusion

In this work we have proposed an algebraically motivated way to discretize the AdS/CFT correspondence. The procedure of replacing real or complex spacetimes by $\mathbb{Q}_p$ introduces a nontrivial discrete bulk and boundary structure while still preserving many desirable features of the correspondence. The boundary conformal field theory lives on an algebraic curve in both the ordinary and non-archimedean examples; the $\mathrm{P}^1(\mathbb{Q}_p)$ theory naturally enjoys the p-adic analogue of the familiar global conformal symmetry, $\mathrm{PGL}(2, \mathbb{Q}_p)$. This same group comprises the isometries of the lattice bulk spacetime $T_p = \mathrm{PGL}(2, \mathbb{Q}_p)/\mathrm{PGL}(2, \mathbb{Z}_p)$, a maximally symmetric coset space analogous to Euclidean AdS.

In analogy with the BTZ black hole and higher genus examples in AdS$_3$, higher genus bulk spaces in the p-adic case are obtained by Schottky uniformization. One takes quotients of the geometry by p-adic Schottky groups $\Gamma \subset \mathrm{PGL}(2, \mathbb{Q}_p)$, producing Mumford curves at the boundary. These curves holographically correspond to bulk geometries consisting of discrete black holes, which appear automatically and do not need to be put in by hand.

Having found a discretization which does not break any symmetries of the problem, we then proposed one way of obtaining a holographic tensor network from a Bruhat–Tits tree. We roughly identify the tree as a space of discrete geodesics in the network. Following Pastawski *et al.*'s holographic error-correcting code, the entanglement entropy of a deleted region is reproduced by counting geodesic lengths in the bulk. This perspective puts a stronger notion of bulk geometry into tensor networks, and suggests that the p-adic systems considered here may be closer to tensor network models than their archimedean counterparts. This construction might have further applications in entangled bulk states, nongeometric bulk states, and other more exotic features of quantum gravity not present in many existing tensor network models.

After discrete bulk Hilbert spaces in tensor networks, we then turned our attention to continuous Hilbert spaces of scalar fields in the tree. In the semiclassical analysis, massless and massive scalar solutions to the lattice model couple naturally to CFT operators at the boundary, just as in the archimedean case. We identified boundary/bulk propagators in the discrete analog of empty AdS, as well as in the p-adic BTZ black hole; the method of images can be used to generalize these results to arbitrary higher-genus bulk backgrounds. We are led to believe that the semiclassical physics of the bulk "gravity" theory is dual to an exotic conformal field theory living on the fractal p-adic boundary. At the present time, little is known about these p-adic conformal field theories outside of p-adic string theory; we hope the connection to holography may draw attention to this area. Viewed as a renormalization scale, we have shown that moving up the

tree corresponds to exact course graining of boundary mode expansions. The intimate relation between conformal symmetry, AdS geometry, and renormalization still holds in this entirely discrete setting.

Motivated by the tensor network models, we suggest that the entanglement entropy of regions of the field theory is computed by the unique geodesic lengths in the bulk space. While as of yet we have no formal proof in the free-boson field theory, a number of arguments have been presented which support this conjecture. Under very specific circumstances, it might even be possible to learn certain properties of the archimedean entanglement entropies from their corresponding p-adic counterparts with the help of adelic formulas.

While we have established some essential features of p-adic holography, ranging from algebraic curves to tensor networks and from bulk/boundary propagators and renormalization scales to entanglement, much about these exotic systems remains to be understood. We propose a number of ideas to be explored in future work.

One major ingredient missing from our story is a proper description of (and quantization of) the gravitational degrees of freedom. The bulk geometries (with or without black holes in the interior) can loosely be described as p-adic discretizations of asymptotically AdS spacetimes. One way to add dynamical metric degrees of freedom without spoiling the asymptotic behavior might be to make the edge lengths of the Bruhat–Tits tree dynamical. The p-adic version of empty AdS might correspond to a solution with uniform edge lengths like the system considered here; thermal or black hole states seem to require topology change in the interior.

If we believe that the full quantum gravity Hilbert space of the interior involves fluctuating edge lengths and graph topology, one might ask if tensor network models could be adapted to this picture. More complicated tensor networks might be used to study objects such as black holes, EPR pairs, and nongeometric states. The role of planarity of the tensor network may play an important role in this story.

From the point of view of the p-adic conformal field theory, one might ask for more interesting examples than the free boson. We have already offered some speculations about higher spin fields based on representation theory of the p-adic conformal group; it would be nice to formulate these models explicitly and search for interesting gravity duals. Additionally, the models we have studied so far do not appear to have extended conformal symmetry or a central charge. These important ingredients of 1+1 dimensional CFT's might appear with the more careful inclusion of finite extensions of $\mathbb{Q}_p$. These finite extensions might also be linked to the passage to Lorentzian signature.

We finally address future work for the entanglement entropy in a p-adic holographic theory. As already mentioned, the single and multiple interval entanglement entropies will likely require a detailed replica computation. This may be possible through a more detailed study of branched covers of the p-adic plane as Mumford curves. With entanglement entropies in hand, one might ask for new and old proofs of entropy

inequalities; these are expected to be simplified by the ultrametric nature of the p-adics. Finally, it remains to be seen how much can be learned about real AdS/CFT from studying these systems adelically over every prime.

Note added

As this work was being completed, we became aware of [29], which treats similar ideas from a somewhat different viewpoint, and in which some of our results in §4.1–4.3 were independently obtained.

Acknowledgements

Appendices

A p-adic integration

Here we review some aspects of p-adic integration, including basic properties and examples, the Fourier transform, and the p-adic gamma function Γ_p. A more comprehensive review is found in [10]. For formal proofs, as well as extensive integration tables, the reader may consult [55].

As already discussed, the unique additive Haar measure dx on $\mathbb{Q}_p$ is normalized so that

$$\int_{\mathbb{Z}_p} dx = 1. \tag{A.1}$$

To find the volume of the set B^r, which consists of $x \in \{\mathbb{Q}_p, |x|_p \leq p^r\}$, we may scale the measure and

reduce this to the integral above on $\mathbb{Z}_p$ as:

$$\int_{B^r} dx = p^r \int_{\mathbb{Z}_p} dx = p^r. \tag{A.2}$$

As $r \to \infty$, the volume diverges as in the real case. Compactifying the point at infinity amounts to switching from the Haar measure to the Patterson-Sullivan measure $d\mu_0(x)$; these measures agree on $\mathbb{Z}_p$ and differ in the complement by $d\mu_0(x) = dx/|x|_p^2$.

With this measure the volume is computed with a change of variables:

$$\int_{\mathbb{Q}_p} d\mu_0(x) = \int_{\mathbb{Z}_p} dx + \int_{\mathbb{Q}_p - \mathbb{Z}_p} |x|_p^{-2} dx \tag{A.3}$$

$$= 1 + \frac{1}{p} \int_{\mathbb{Z}_p} du, \quad u = \frac{1}{px}, \quad du = \frac{p\, dx}{|x|_p^2} \tag{A.4}$$

$$= \frac{p+1}{p}. \tag{A.5}$$

A large class of elementary integrals may be evaluated using these methods; see the above references for complete details.

We now turn our attention to the p-adic Fourier transform of a function $f(x) : \mathbb{Q}_p \to \mathbb{C}$. As discussed in section 4.2.1, this involves integrating the function against the additive character $\chi(x) = e^{2\pi i \{kx\}}$ over all $\mathbb{Q}_p$. This generates a new complex valued function in terms of the p-adic momentum $k \in \mathbb{Q}_p$:

$$\widetilde{f}(k) = \int_{\mathbb{Q}_p} \chi(kx) f(x) dx, \tag{A.6}$$

$$f(x) = \int_{\mathbb{Q}_p} \chi(-kx) \widetilde{f}(k) dk. \tag{A.7}$$

The analogy with the real Fourier transform should be clear. In practice evaluating this kind of integral often requires one to divide $\mathbb{Q}_p$ into spheres consisting of points with $|x|_p = p^n$ and performing the integral on each sphere. This can be seen in the example:

$$\int_{B^r} \chi(kx) dx = \begin{cases} p^r, & |k|_p \leq p^{-r} \\ 0, & \text{otherwise.} \end{cases} \tag{A.8}$$

As in the real case, one may find tables with numerous p-adic Fourier transforms of elementary functions in the literature.

The final integral expression is that of the Gelfand-Graev-Tate Γ function:

$$\Gamma_p(\alpha) = \int_{\mathbb{Q}_p} \chi(x)|x|_p^{\alpha-1} dx = \frac{1-p^{s-1}}{1-p^{-s}}. \tag{A.9}$$

This function has some similar properties to the ordinary gamma function. It is fairly ubiquitous in certain p-adic integral calculations, and we refer the reader to literature on p-adic string theory for details.

B p-adic differentiation

As already discussed, complex fields living on the boundary $\mathrm{P}^1(\mathbb{Q}_p)$ are maps

$$f(x) : \mathrm{P}^1(\mathbb{Q}_p) \to \mathbb{C}. \tag{B.1}$$

In the archimedean case of 2d conformal field theory, we have $f(z, \bar{z}) : \mathrm{P}^1(\mathbb{C}) \to \mathbb{C}$ and it makes sense to define holomorphic and antiholomorphic derivatives $\frac{\partial f}{\partial z}$ and $\frac{\partial f}{\partial \bar{z}}$. In the p-adic case, analogous differentiation expressions no longer make sense are we would be dividing a complex number by a p-adic number and these fields have different topologies.

The only notion of derivative we may use is the *Vladimirov derivative* [55, 21], and it can be thought of as a nonlocal pseudo-differential operator. Roughly speaking, this operation is the p-adic analog of Cauchy's Differentiation Formula in which the derivative of a function at a point is expressed as a weighted integral of the function over a curve. It is also know as a *normal derivative* [58] in the context of the p-adic string where it is interpreted as the derivative of the embedding coordinates X^μ normal to the boundary of the worldsheet. Becaues this operator is defined on $\mathbb{Q}_p$ without any reference to an embedding or worldsheet, we opt to refer to it as a Vladimirov derivative. The nth Vladimirov derivative is defined by

$$\partial_{(p)}^n f(x) = \int_{\mathbb{Q}_p} \frac{f(x') - f(x)}{|x' - x|_p^{n+1}} dx'. \tag{B.2}$$

Some authors may choose a different normalization in front of this integral; usually in the form of p-adic gamma functions. At first sight the expression above may not resemble any familiar notions of differentiation. We may see this as a good notion for derivative in two ways; in the case of the p-adic string this expression is the limit of the normal derivative on T_p as we go to the boundary, as shown in [58]. We may also compute the Vladimirov derivative of some special p-adic functions and compare with the real case. This is done in the following section.

B.1 Examples

We wish to first compute the derivative of the additive character, $\chi(kx)$. This function is the p-adic analog of a plane wave with momentum k, so we expect it to be an eigenfunction of the derivative with eigenvalue related to k.

$$\partial_{(p)}^n \chi(kx) = \int_{\mathbb{Q}_p} \frac{\chi(kx') - \chi(kx)}{|x' - x|_p^{n+1}} dx'. \tag{B.3}$$

Using the properties of the additive Haar measure of $\mathbb{Q}_p$, we can shift the integration measure,

$$y = k(x' - x), \quad dy = |k|_p dx' \tag{B.4}$$

and simplify the integral

$$\int_{\mathbb{Q}_p} \frac{\chi(kx') - \chi(kx)}{|x' - x|_p^{n+1}} dx' \tag{B.5}$$

$$= |k|_p^n \int_{\mathbb{Q}_p} \frac{\chi(y + kx) - \chi(kx)}{|y|_p^{n+1}} dy \tag{B.6}$$

$$= |k|_p^n \chi(kx) \int_{\mathbb{Q}_p} \frac{\chi(y) - 1}{|y|_p^{n+1}} dy. \tag{B.7}$$

Where we used the additive property of the character to extract the x dependence. The integral appears to diverge at $y \sim 0$; this divergence is actually canceled by the numerator and can be seen by introducing an infrared cutoff. Regularization of this integral is discussed in [4] and [26]. The result is

$$\int_{\mathbb{Q}_p} \frac{\chi(y) - 1}{|y|_p^{n+1}} dy = \frac{1 - p^{-n-1}}{1 - p^n} = \Gamma_p(-n), \tag{B.8}$$

where we have used the definition of the p-adic gamma function in Eq. (A.9). So the end result is

$$\partial_{(p)}^n \chi(kx) = \Gamma_p(-n)|k|_p^n \chi(kx). \tag{B.9}$$

Up to the factor of the gamma function (which could be absorbed into the normalization of the derivative,) we see the additive character $\chi(kx)$ is an eigenfunction of the Vladimirov derivative with the eigenvalue given by the p-adic norm of its "momentum."

Another example we may wish to compute is the nth derivative of $|x|_p^s$ for some $s \in \mathbb{C}$. This may be most easily be computed by Fourier transform and serves as an example of an alternative representation

of the Vladimirov derivative:

$$\partial_{(p)}^n |x|_p^s = \int \chi(-kx)|k|_p^n \widetilde{|x|^s}_p \, dk \tag{B.10}$$

where $\widetilde{|x|^s}_p$ is the p-adic Fourier transform of $|x|_p^s$, given in [60, 55]:

$$\widetilde{|x|^s}_p = \int \chi(kx)|x|_p^s \, dx = \Gamma_p(s+1)|k|_p^{-s-1} \tag{B.11}$$

everywhere it is defined. Applying this formula twice to the derivative we wish to compute, we arrive at

$$\partial_{(p)}^n |x|_p^s = \Gamma_p(s+1)\Gamma_p(n-s)|x|_p^{s-n}, \tag{B.12}$$

which should resemble the ordinary n^{th} derivative of a polynomial function.

References

[1] A. Almheiri, X. Dong, and D. Harlow, *Bulk locality and quantum error correction in AdS/CFT*, J. of High Energy Physics **2015**, no. 4 (2015): 1–34.

[2] M. Bañados, C. Teitelboim, J. Zanelli, *Black hole in three-dimensional spacetime*, Phys. Rev. Lett. Vol.69 (1992) N.13, 1849–1851.

[3] N. Bao, C. J. Cao, S. M. Carroll, A. Chatwin-Davies, N. Hunter-Jones, J. Pollack, and G. N. Remmen, *Consistency conditions for an AdS multiscale entanglement renormalization ansatz correspondence*, Physical Review D **91**, no. 12 (2015): 125036.

[4] A. Kh. Bikulov and A. P. Zubarev, *On one real basis for $L^2(\mathbb{Q}_p)$*, preprint arXiv:1504.03624v1 (2015).

[5] N. Bao, S. Nezami, H. Ooguri, B. Stoica, J. Sully, and M. Walter, *The holographic entropy cone*, JHEP **1509**, no. 130 (2015): 130.

[6] D. Birmingham, C. Kennedy, S. Sen, A. Wilkins, *Geometrical finiteness, holography, and the Bañados-Teitelboim-Zanelli black hole*, Phys. Rev. Lett. Vol.82 (1999) N.21, 4164–4167.

[7] J. F. Boutot, H. Carayol, *Uniformization p-adique des courbes de Shimura: les théorèmes de Cerednik et de Drinfeld*, in "Courbes modulaires et courbes de Shimura" (Orsay, 1987/1988). Astérisque Vol.196–197 (1991) N.7 45–158.

[8] R. Bowen. *Hausdorff dimension of quasi-circles*, Publ. Math. IHES Vol.50 (1979) 11–25.

[9] P. E. Bradley, *Cyclic coverings of the p-adic projective line by Mumford curves*, Manuscripta Mathematica **124**, no. 1 (2007): 77–95.

[10] L. Brekke and P. G. O. Freund, *p-adic numbers in physics*, Physics Reports **233**, no. 1 (1993), pp. 1–66.

[11] L. Brekke, P. G. O. Freund, M. Olson, and E. Witten, *Non-archimedean string dynamics*, Nuclear Physics B **302**, no. 3 (1988): 365–402.

[12] P. Calabrese and J. Cardy, *Entanglement entropy and quantum field theory*, Journal of Statistical Mechanics: Theory and Experiment **2004**, no. 06 (2004): P06002.

[13] P. Calabrese and J. Cardy, *Entanglement entropy and conformal field theory*, Journal of Physics A: Mathematical and Theoretical **42**, no. 50 (2009): 504005.

[14] R. D. Canary, *Ends of hyperbolic 3-manifolds*, J. American Math. Soc. Vol.6 (1993) N.1, 1–35.

[15] A. Carey, M. Marcolli, A. Rennie, *Modular index invariants of Mumford curves*, in "Noncommutative geometry, arithmetic, and related topics," pp. 31–73, Johns Hopkins Univ. Press, Baltimore, 2011.

[16] H. Casini, M. Huerta, *Universal terms for the entanglement entropy in 2+1 dimensions*, *Nuclear Physics B* **764**, (2007) pp. 183–201

[17] B. Casselman, *The Bruhat–Tits tree of* SL(2), unpublished notes (available online).

[18] C. Consani, M. Marcolli, *Noncommutative geometry, dynamics, and ∞-adic Arakelov geometry*, Selecta Math. (N.S.) Vol.10 (2004) N.2, 167–251.

[19] C. Consani, M. Marcolli, *Spectral triples from Mumford curves*, Int. Math. Res. Not. (2003) N.36, 1945–1972.

[20] C. Consani, M. Marcolli, *New perspectives in Arakelov geometry*, in "Number theory," pp. 81–102, CRM Proc. Lecture Notes, Vol. 36, Amer. Math. Soc., 2004.

[21] B. Dragovich, A. Yu. Khrennikov, S. V. Kozyrev, and I. V. Volovich, *On p-adic Mathematical Physics*, preprint arXiv:0904.4205v1 (2009).

[22] T. Faulkner, *The entanglement Rényi entropies of disjoint intervals in AdS/CFT*, preprint arXiv:1303.7221 (2013).

[23] P. G. O. Freund and E. Witten, *Adelic string amplitudes*, Physics Letters B **199**, no. 2 (1987): 191–194.

[24] P. G. O. Freund and M. Olson, *Non-archimedean strings*, Physics Letters B **199**, no. 2 (1987): 186–190.

[25] L. Gerritzen, M. van der Put, *Schottky groups and Mumford curves*, Lecture Notes in Mathematics, Vol.817, Springer, 1980.

[26] D. Ghoshal and T. Kawano, "Towards p-adic string in constant B-field," *Nuclear Physics B* **710**, no. 3 (2005), pp. 577–598.

[27] P. Grange, *Deformation of p-adic String Amplitudes in a Magnetic Field*, preprint arXiv:hep-th/0409305 (2004).

[28] M. Grassl, T. Beth, and M. Rötteler, *On optimal quantum codes*, International Journal of Quantum Information **2**, no. 01 (2004): 55–64.

[29] S. S. Gubser, J. Knaute, S. Parikh, A. Samberg, and P. Witaszczyk, *p-adic AdS/CFT*, preprint arXiv:1605.01061 (2016).

[30] C. Holzhey, F. Larsen, and F. Wilczek, *Geometric and Renormalized Entropy in Conformal Field Theory*, Nuclear Physics B **424** (1994) pp.443–467

[31] K. Krasnov, *Holography and Riemann surfaces*, Adv. Theor. Math. Phys. Vol.4 (2000) N.4, 929–979.

[32] N. Koblitz, *p-adic numbers, p-adic analysis, and zeta-functions*, Springer Science & Business Media **58** (2012).

[33] J. Maldacena and A. Strominger, *AdS$_3$ black holes and a stringy exclusion principle*, J. High Energy Phys. 1998, no. 12, Paper 5, 24 pp.

[34] J. Maldacena and L. Susskind, *Cool horizons for entangled black holes*, Fortschritte der Physik **61**, no. 9 (2013): 781–811.

[35] Yu.I. Manin, V. Drinfeld, *Periods of p-adic Schottky groups*, J. Reine Angew. Math. Vol.262-263 (1973) 239–247.

[36] Yu.I. Manin, *Three-dimensional hyperbolic geometry as ∞-adic Arakelov geometry*, Invent. Math. Vol.104 (1991) N.2, 223–243.

[37] Yu.I. Manin, *Closed fibers at infinity in Arakelov's geometry*, preprint PAM-479, Center for Pure and Applied Mathematics, University of California Berkeley, 1989.

[38] Yu.I. Manin, *Reflections on arithmetical physics*, in "Conformal invariance and string theory," pp. 293–303, Perspect. Phys., Academic Press, 1989.

[39] Yu.I. Manin, *p-adic automorphic functions*, Journ. of Soviet Math. Vol.5 (1976) 279–333.

[40] Yu.I. Manin, M. Marcolli, *Holography principle and arithmetic of algebraic curves*, Adv. Theor. Math. Phys. Vol.5 (2001) N.3, 617–650.

[41] M. Marcolli, *Arithmetic Noncommutative Geometry*, University Lecture Series, Vol.36, American Mathematical Society, 2005.

[42] E. Melzer, *Nonarchimedean conformal field theories*, Int. J. of Modern Physics A **4**, no. 18 (1989), pp. 4877–4908.

[43] D. Mumford, *An analytic construction of degenerating curves over complete local rings*, Compositio Math. Vol.24 (1974) 129–174.

[44] J. Neukirch, *Algebraic number theory*, Springer Science & Business Media **322** (2013).

[45] F. Pastawski, B. Yoshida, D. Harlow, and J. Preskill, *Holographic quantum error-correcting codes: toy models for the bulk/boundary correspondence*, preprint arXiv:1503.06237 (2015).

[46] G. Parisi, *On p-adic functional integrals*, Modern Physics Letters A, Vol. 3, No. 6 (1988), pp. 639–643

[47] M. van der Put, *Discrete groups, Mumford curves and theta functions*, Ann. Fac. Sci. Toulouse Math. (6), Vol.1 (1992) N.3, 399–438.

[48] S. Ryu and T. Takayanagi, *Holographic derivation of entanglement entropy from AdS/CFT*, Phys. Rev. Lett. **96**, no. 18 (2006): 181602.

[49] P. J. Sally Jr., *An introduction to p-adic fields, harmonic analysis, and the representation theory of SL(2)*, Letters in Mathematical Physics **46**, no 1 (1998): 1–47.

[50] B. L. Spokoiny, *Quantum geometry of non-archimedean particles and strings*, Physics Letters B **208**, no. 3 (1988): 401–405.

[51] M. Srednicki, *Entropy and Area*, Phys.Rev.Lett. **71** (1993) 666-669

[52] B. Swingle, *Entanglement renormalization and holography*, Phys. Rev. D **86**, no. 6 (2012): 065007.

[53] L. Takhtajan, P. Zograf, *On uniformization of Riemann surfaces and the Weyl-Petersson metric on Teichmüller and Schottky spaces*, Math. USSR Sbornik, 60 (1988) 297–313.

[54] G. Vidal, *Class of quantum many-body states that can be efficiently simulated*, Phys. Rev. Lett. **101**, no. 11 (2008): 110501.

[55] V. S. Vladimirov, *Tables of Integrals of Complex-valued Functions of p-Adic arguments*, preprint arXiv:math-ph/9911027v1 (1999).

[56] V. S. Vladimirov, I. V. Volovich, and E. I. Zelenov, eds. *p-adic analysis and mathematical physics*, Vol. 1. World Scientific, 1994.

[57] E. Witten, *Anti-de Sitter space and holography*, preprint arXiv:hep-th/9802150 (1998).

[58] A. V. Zabrodin, *Non-archimedean strings and Bruhat–Tits trees*, Communications in Mathematical Physics **123**, no. 3 (1989), pp. 463–483.

[59] L. O. Chekhov, A. D. Mironov, and A. V. Zabrodin, *Multiloop calculations in p-adic string theory and Bruhat–Tits Trees*, Communications in Mathematical Physics **125**, (1989), pp. 675–711.

[60] R. B. Zhang, *Lagrangian formulation of open and closed p-adic strings*, Physics Letters B **209**, no. 2–3 (1988), pp. 229–232.